Nuclear Excited Studied by proton scattering With a High-Resolution Magnetic Spectrometer

Lecture V

Photo Nuclear Reaction of Ultra-High-Energy Cosmic Rays

3537 9704 at https://menti.com

https://www.menti.com/alaivzqmrgqy

Constraints on Symmetry Energy (J and L)

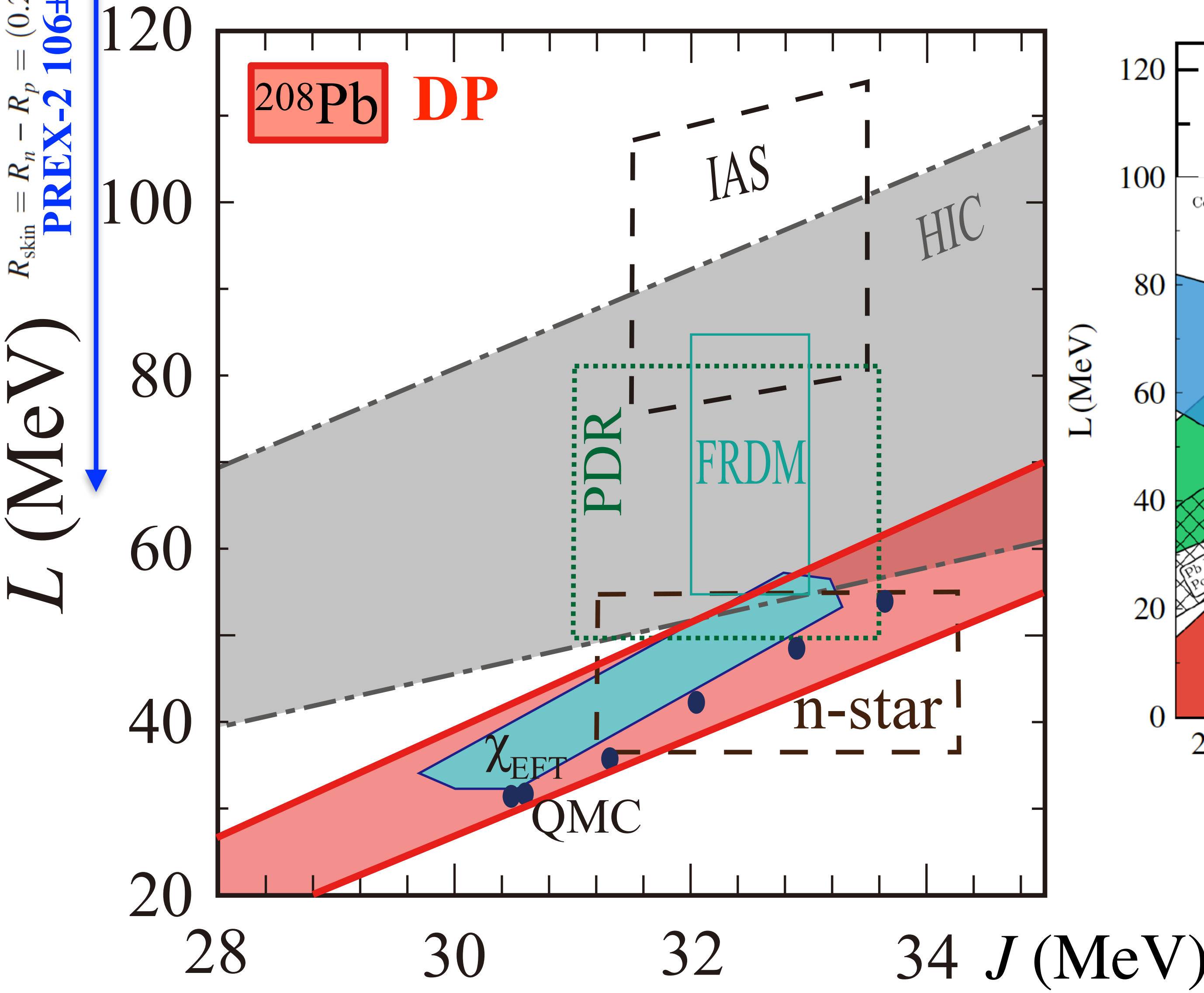

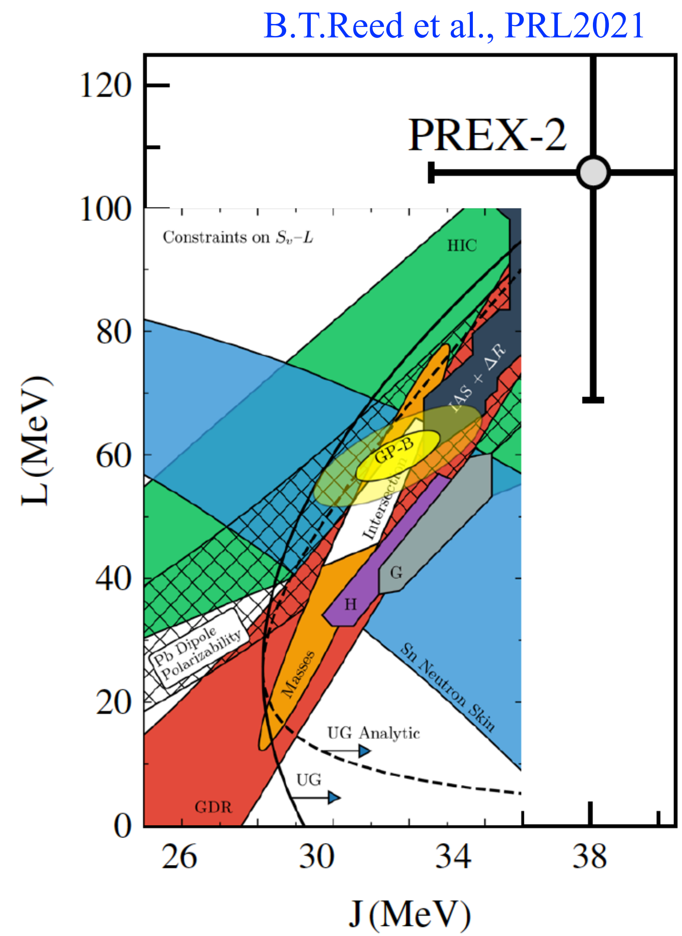

DP: Dipole Polarizability

^{208}Pb AT PRL2011

Neutron Skin Thickness

See e.g. a review paper by James M. Lattimer et al., *Particles* **2023**, *6*, 30–56.

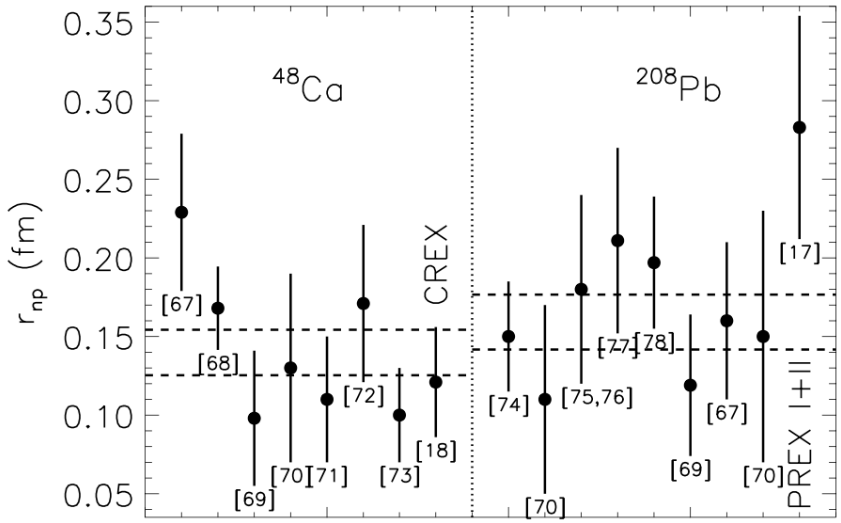

Figure 8. Neutron skin measurements [17,18,70–81] Horizontal dashed lines denote ±1 standard deviatic other than CREX or PREX I+II.

Table 4. ^{208}Pb neutron skin measurements and theoretical predictions with 1σ uncertainties

^{208}Pb Experiment	Reference	r_{np}^{208} (fm)
Coherent $\pi^0\gamma$ production	[77]	$0.15^{+0.03}_{-0.04}$
Pionic atoms	[73]	0.15 ± 0.08
Pion scattering	[73]	0.11 ± 0.06
$\bar{p}$ annihilation	[78,79]	0.18 ± 0.06
Elastic polarized p scattering	[70]	0.16 ± 0.05
Elastic polarized p scattering	[80]	$0.211^{+0.054}_{-0.063}$
Elastic p scattering	[81]	0.197 ± 0.042
Elastic p scattering	[72]	0.119 ± 0.045
Parity-violating e^- scattering (PREX I+II)	[17]	0.283 ± 0.071
^{208}Pb experimental weighted mean		0.166 ± 0.017
Pygmy dipole resonances	[82]	0.180 ± 0.035
r_{np}^{Sn}	[83]	0.175 ± 0.020
Anti-analog giant dipole resonance	[84]	0.216 ± 0.048
Symmetry energy ^{208}Pb	[85]	0.158 ± 0.014
Dispersive optical model	[86]	$0.18^{+0.25}_{-0.12}$
Dispersive optical model	[67]	0.25 ± 0.05
Coupled cluster expansion	[66]	0.17 ± 0.03
r_{np}^{48}	[63,64], this paper	0.128 ± 0.040
α_D^{208}	[62], this paper	0.154 ± 0.019
α_D^{208}	[20,64], this paper	0.188 ± 0.017
^{208}Pb theoretical weighted mean		0.170 ± 0.008

Photo-Reaction of Light Nuclei and Ultra-High-Energy Cosmic Rays

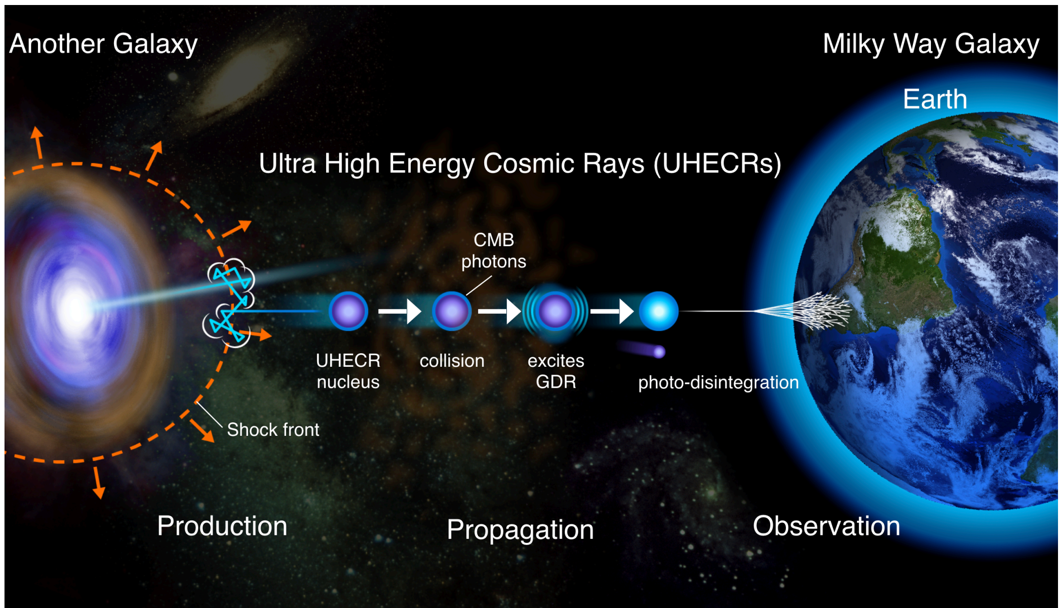

PANDORA

Photo-Absorption of Nuclei and Decay Observation for Reactions in Astrophysics

Ultra High Energy Cosmic Rays (UHECRs)

Primary Cosmic Rays: Flux and Composition

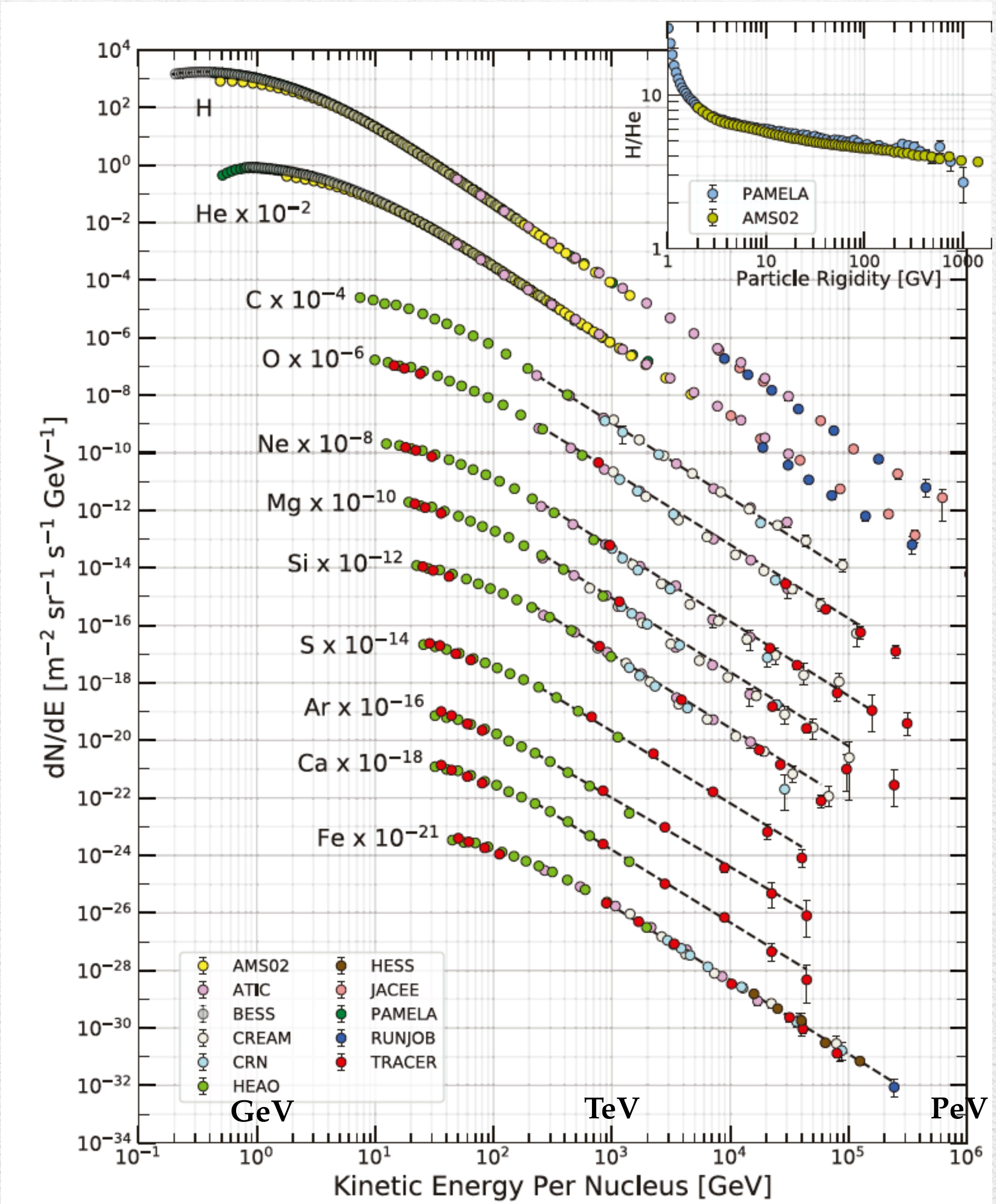

Z	Element	F	Z	Element	F
1	H	550	13–14	Al-Si	0.19
2	He	34	15–16	P-S	0.03
3–5	Li-B	0.40	17–18	Cl-Ar	0.01
6–8	C-O	2.20	19–20	K-Ca	0.02
9–10	F-Ne	0.30	21–25	Sc-Mn	0.05
11–12	Na-Mg	0.22	26–28	Fe-Ni	0.12

composition relative to oxygen at 10.6 GeV/A

[PDG2018]

High Energy Cosmic Rays

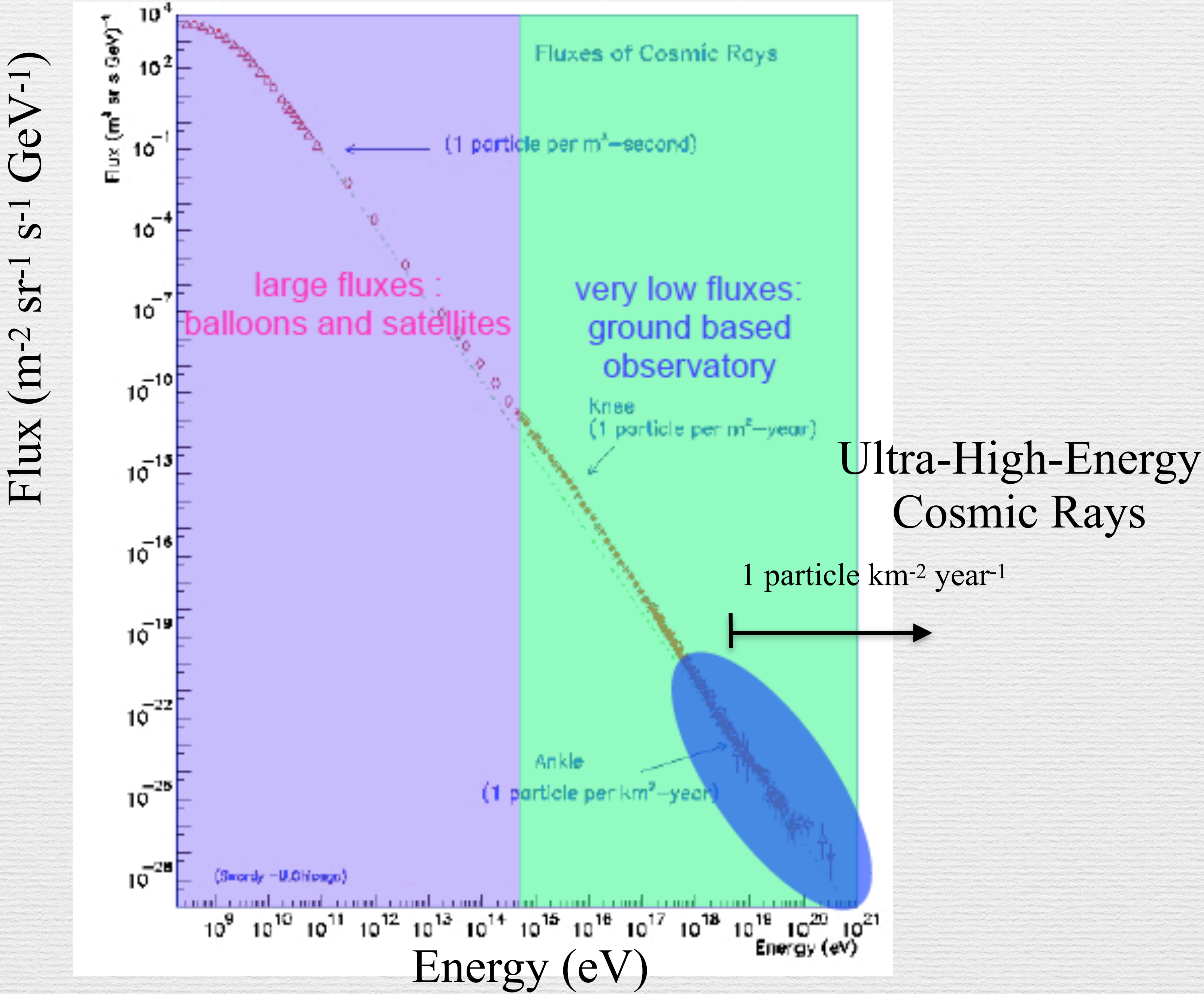

Ultra-High-Energy Cosmic Rays (UHECRs) [PDG2018]

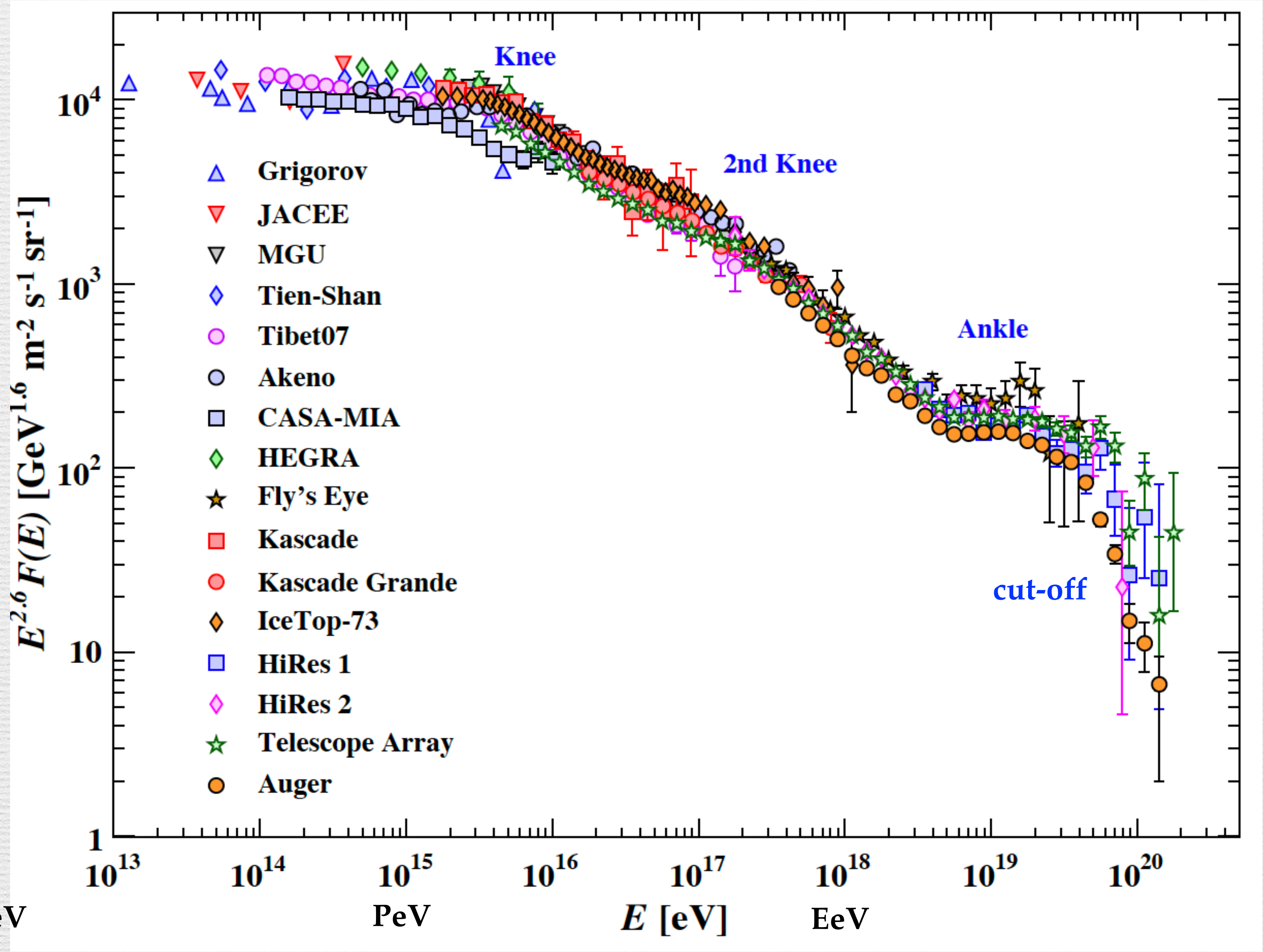

Ultra-High-Energy Cosmic Rays (UHECRs) [PDG2018]

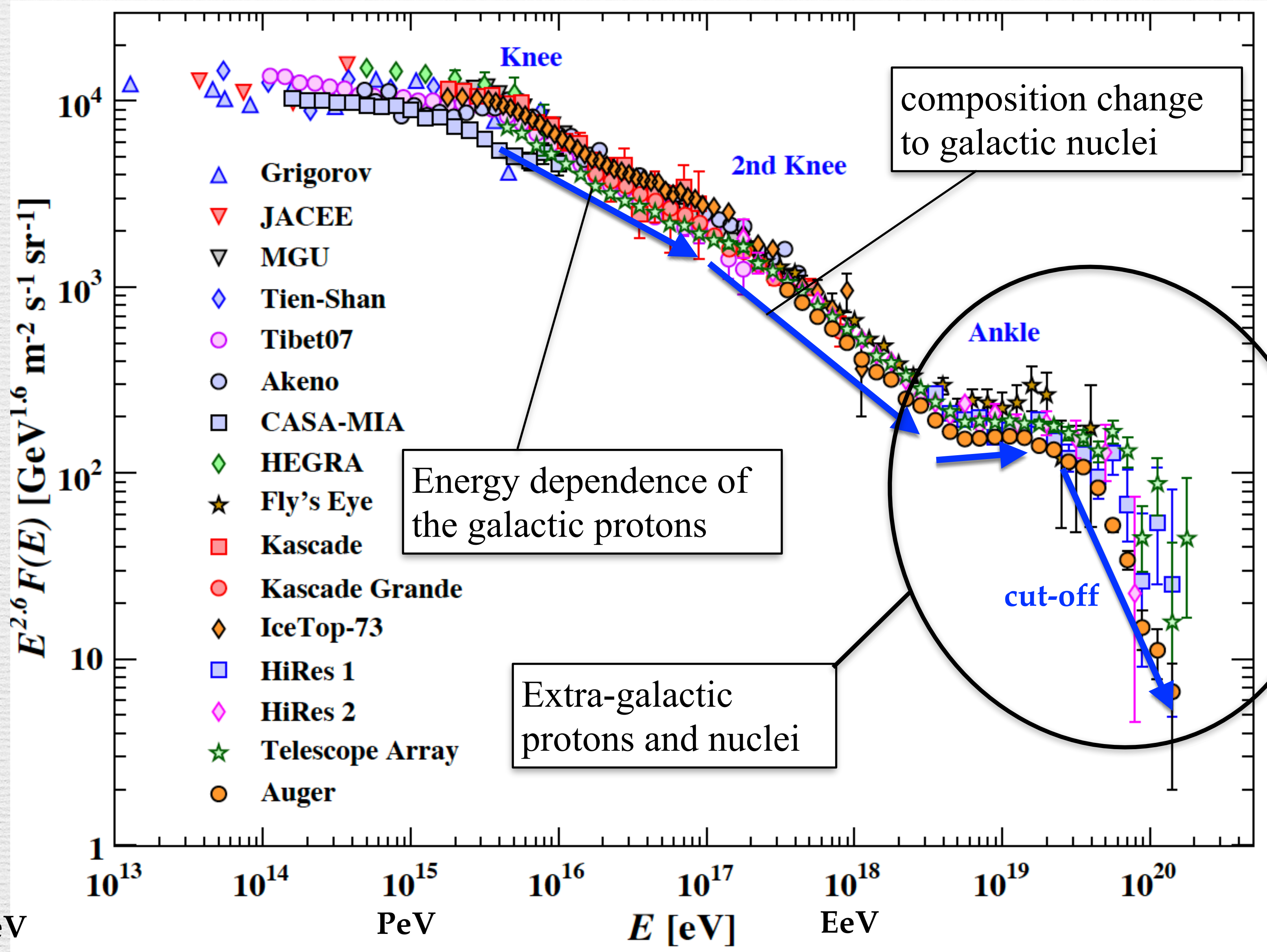

Ultra-High-Energy Cosmic Rays (UHECRs) [PDG2018]

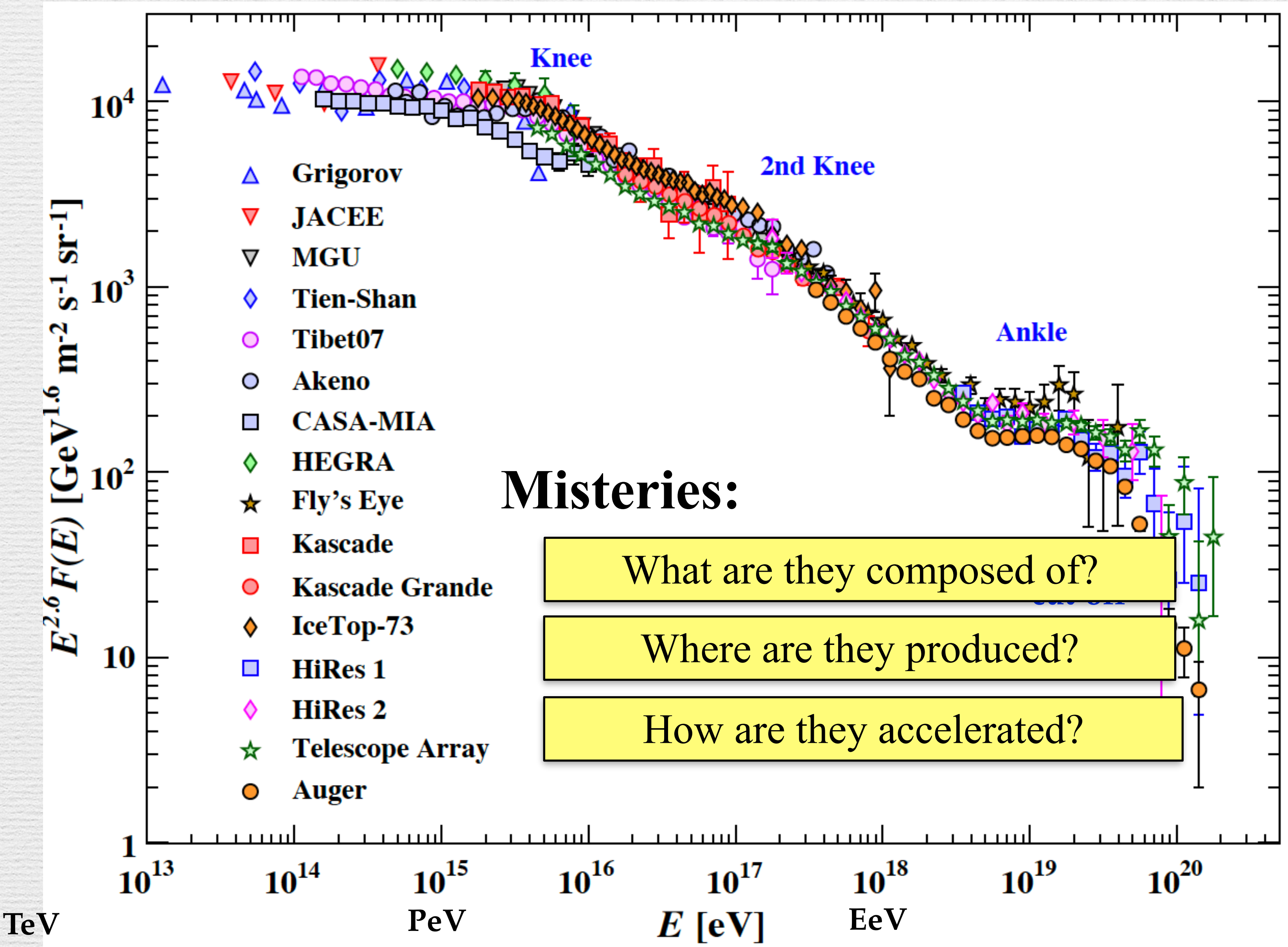

Misteries:

- What are they composed of?
- Where are they produced?
- How are they accelerated?

UHECR Observatories (Auger and TA)

Observation of UHECRs

Extended Air Shower (EAS)

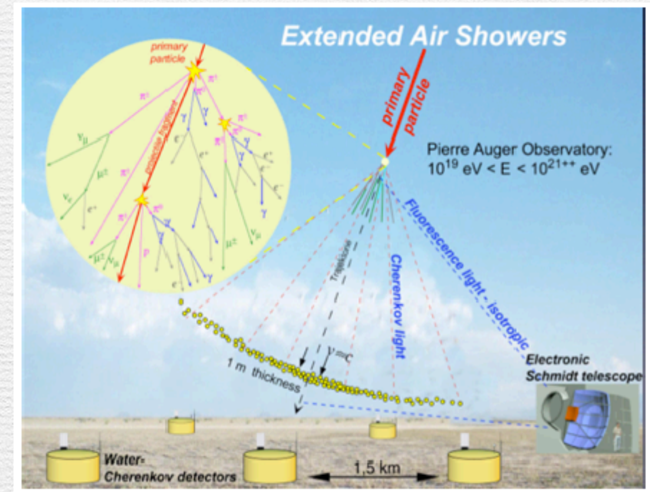

Hadronic process

primarily produces mesons (π or K)

p(A) +A → π, K, and nuclear fragments

$\pi^{\pm} \rightarrow \mu^{\pm} + \nu_{\mu}\ (\overline{\nu_{\mu}})$

$\pi^0 \rightarrow 2\gamma$

$\gamma \rightarrow e^{+}+e^{-}$

$e^{\pm} + A \rightarrow e^{\pm}+A+\gamma$

Electromagnetic Shower

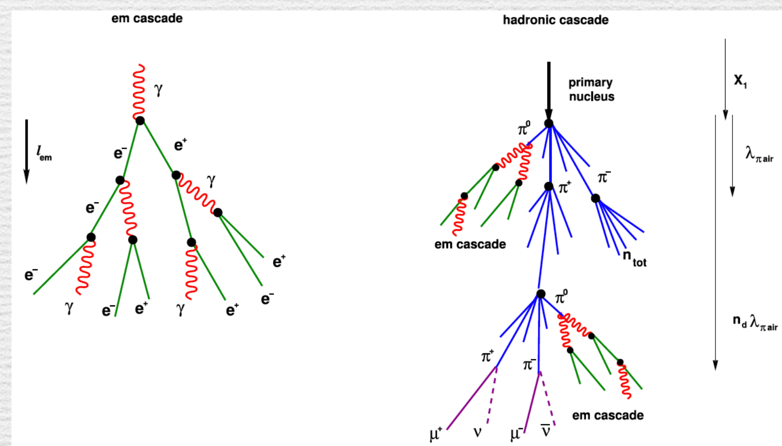

[mol18]

(Osaka Univ. →) Pierre Auger Observatory

Pierre Auger Observatory

[aug15, aug04]

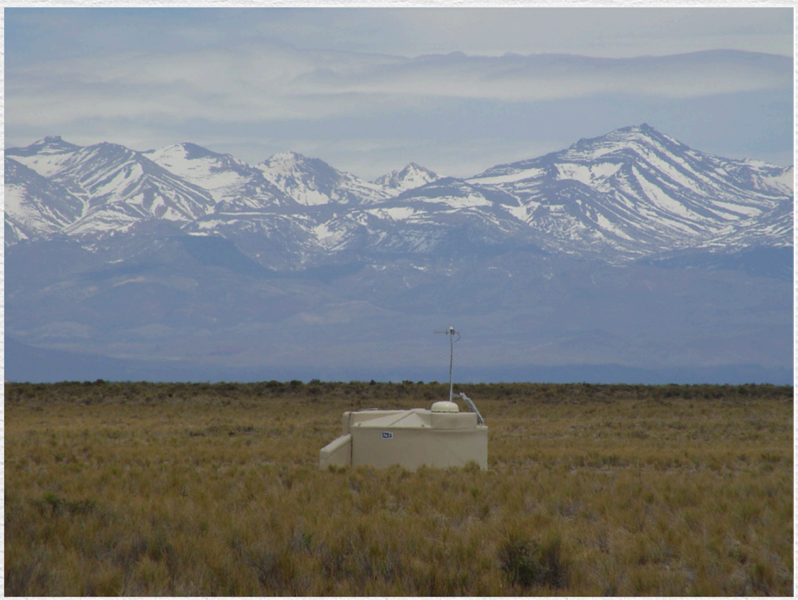

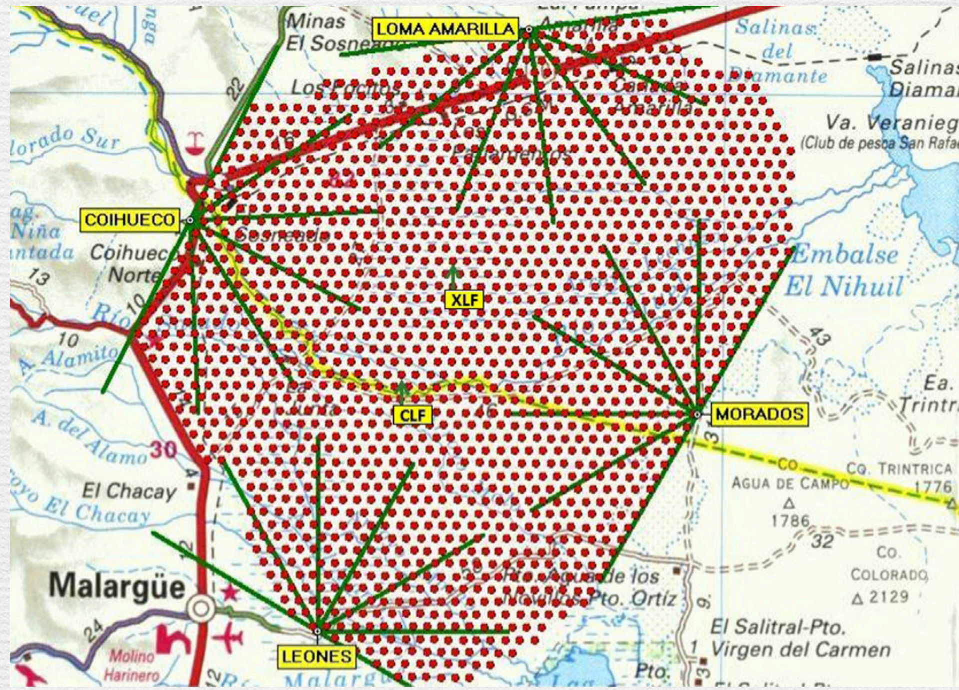

The Pampa Amarilla site (35.1°–35.5° S, 69.0°–69.6° W and 1300–1400 m asl) lies in the south of the Province of Mendoza, Argentina, close to Malargüe (pop. 18 000) and 180 km south west of San Rafael (pop. 100 000). It encompasses an area of 3100 km^2 (see Fig. 1a).

Pierre Auger Observatory

Pierre Auger Observatory
Surface Detector (SD)

[aug04]

3,000 km^2 (~60kmϕ)

1,600 water Cherenkov detectors (SD)
in a polyethylene tank

mean distance 1.5 km on triangular grid

~0.5 SD / km^2

High-purity water
in three-layers of polyolefin liner
(140+28+178μm)

10 m^2 area × 1.2 m depth

Three PMT's

or
Hamamatsu R5921 8″ϕ
Photonis XP1802 9″ϕ

FADC 40 MHz

Time recording calibrated by GPS.
(σ=7.24 ns)

100% running efficiency measured from 2004

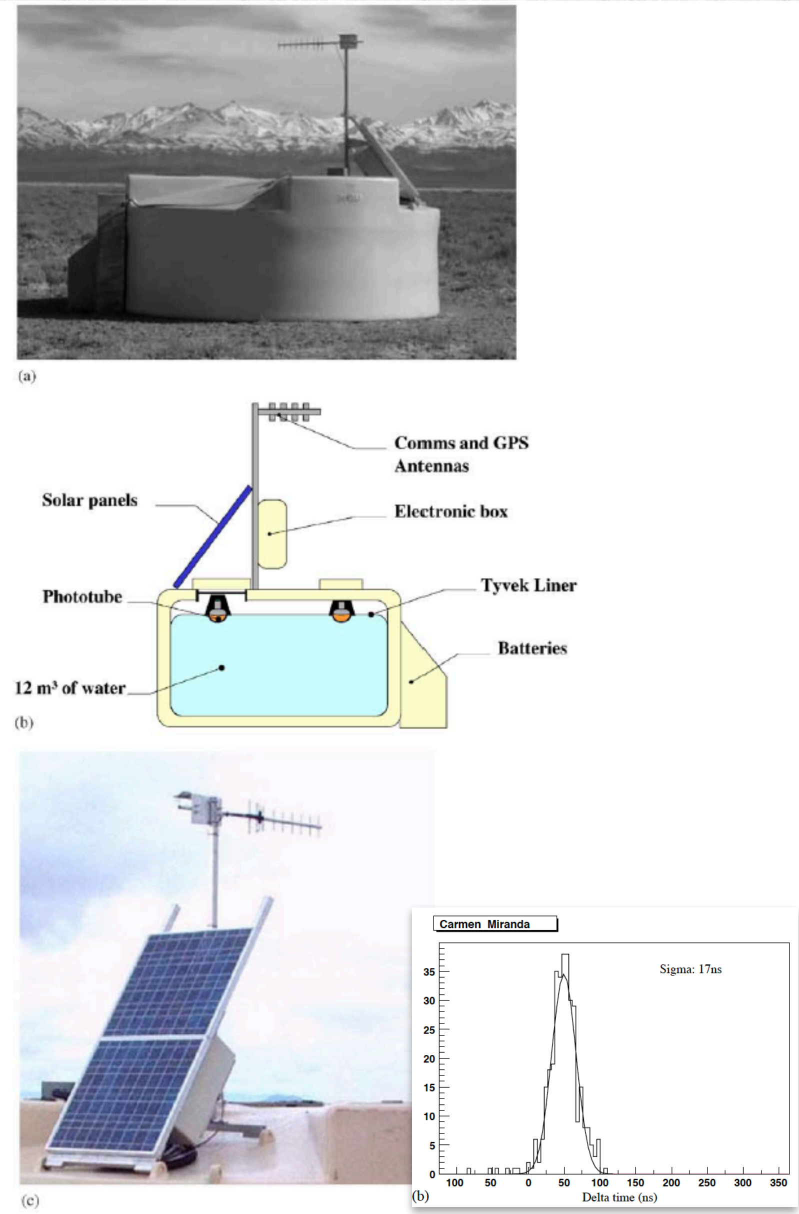

Fig. 2. (a) A photograph of an EA water tank; (b) schematic view of an EA tank; (c) the Yagi antenna and the solar power array.

Pierre Auger Observatory
(Fluorescence Detector) FD

[aug15, aug04]

24 fluorescence detector telescopes at 4 sites

with spherical mirror (3.5m×3.5m)
and (440) PMT camera

30° azimuth×28.6° elevation field of view per telescope

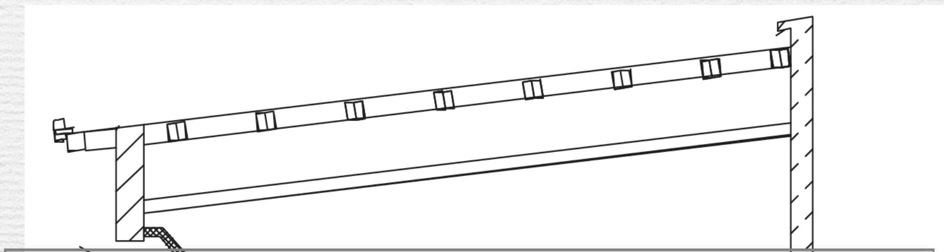

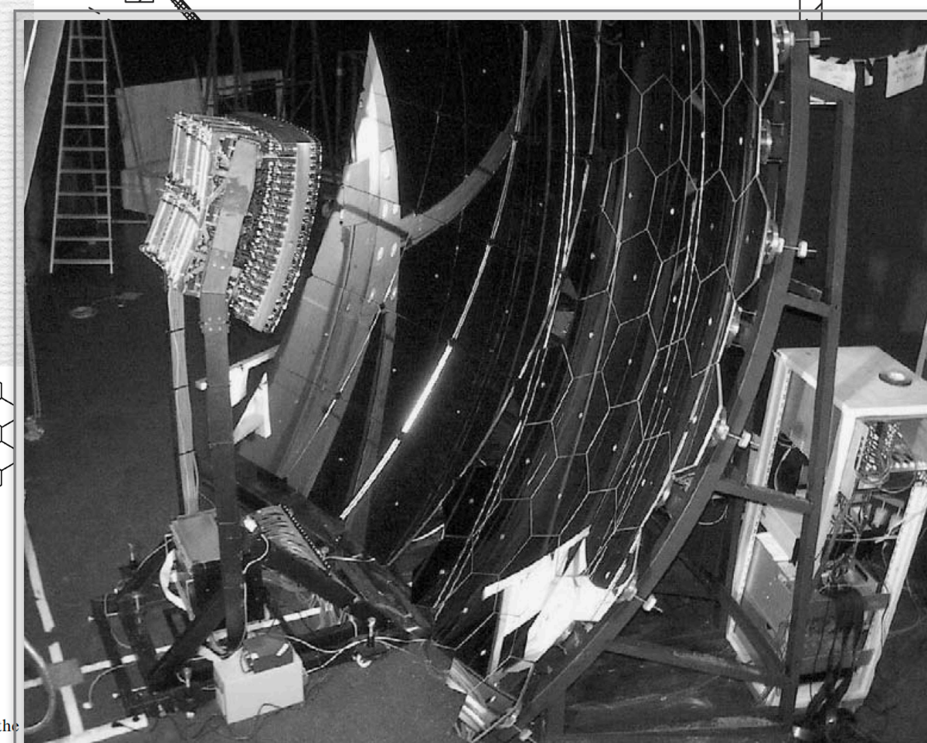

UV light 310-390 nm
fluorescence from nitrogen in the air

Continuous digitization by 10MHz 12 bit ADC

100 Hz recording using sum trigger and threshold (20μsec)

Calibrated by YAG-laser (355nm) from CLF and XLF

~15% running efficiency with clear sky no moon

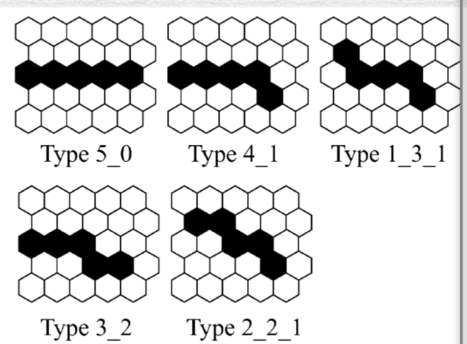

Fig. 8. Basic topological patterns of triggered pixels used in the second level trigger.

(Auger →) Telescope Array

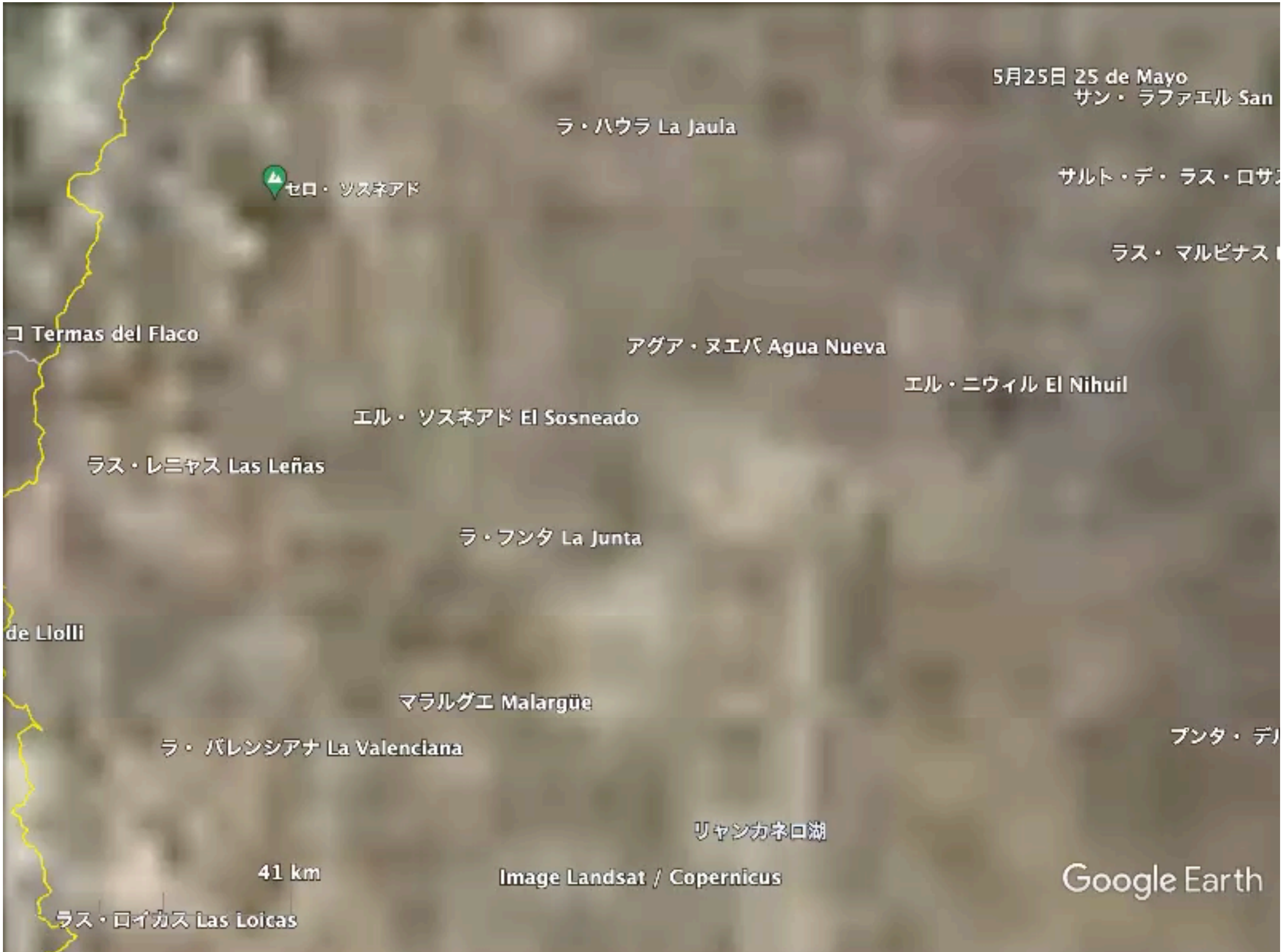

Telescope Array

[tok11, abu12,]

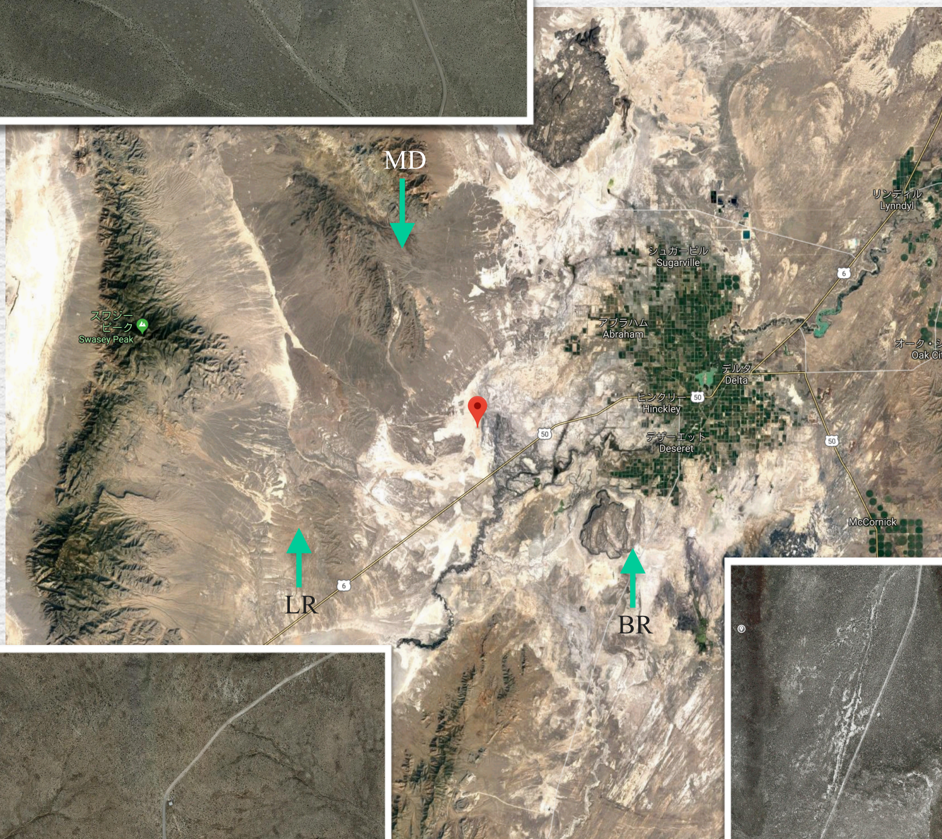

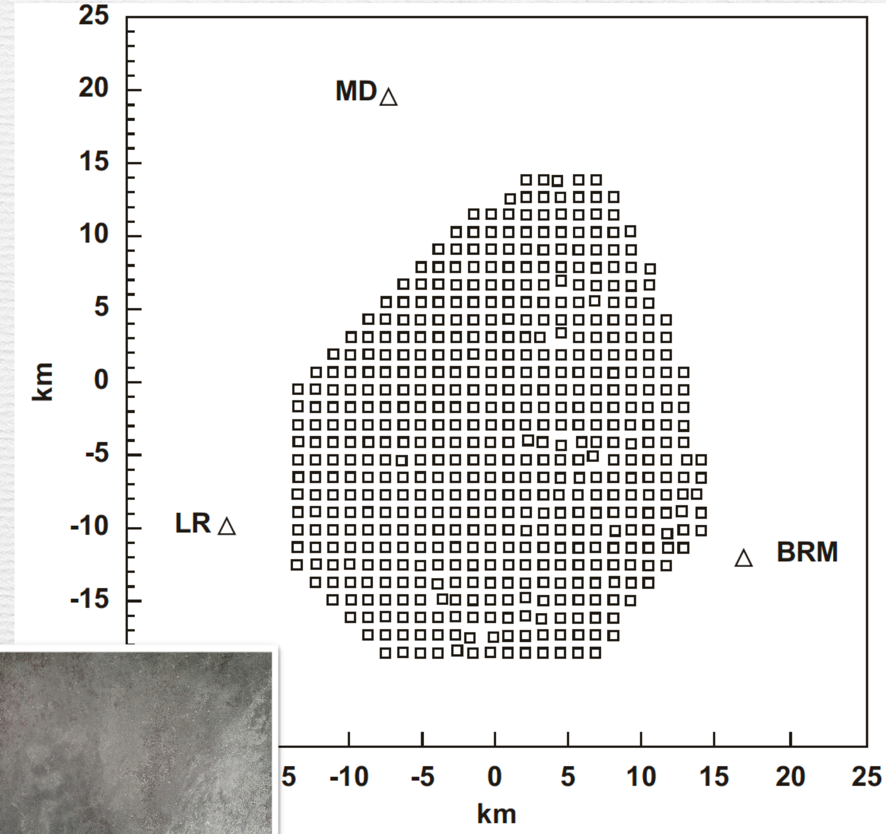

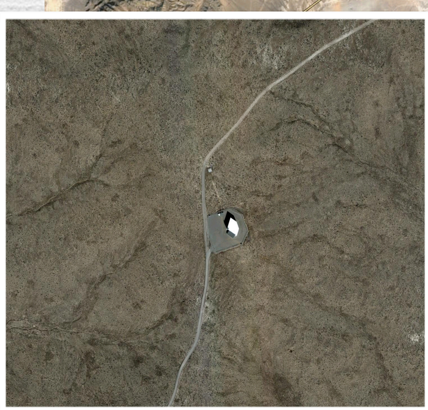

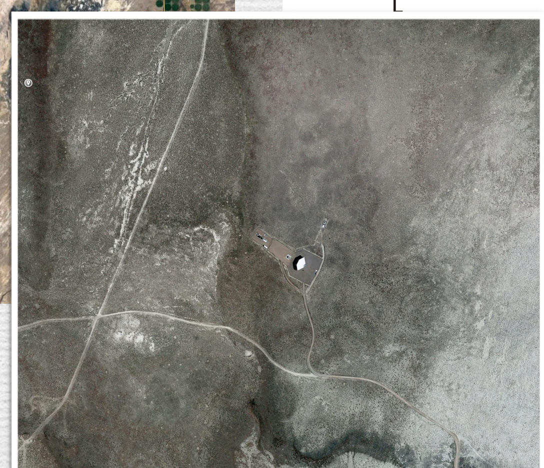

cated in the desert about 1400 m above sea level
and 112.9°W in Millard County, Utah, USA, about
of Salt Lake City. A control center to support

Telescope Array FD

[tok11, abu12,]

12 fluorescence detector telescopes at 3 sites

Primary mirror (3.3mϕ) and (16×16) PMT camera

18° azimuthal 15° elevation field of view / telescope

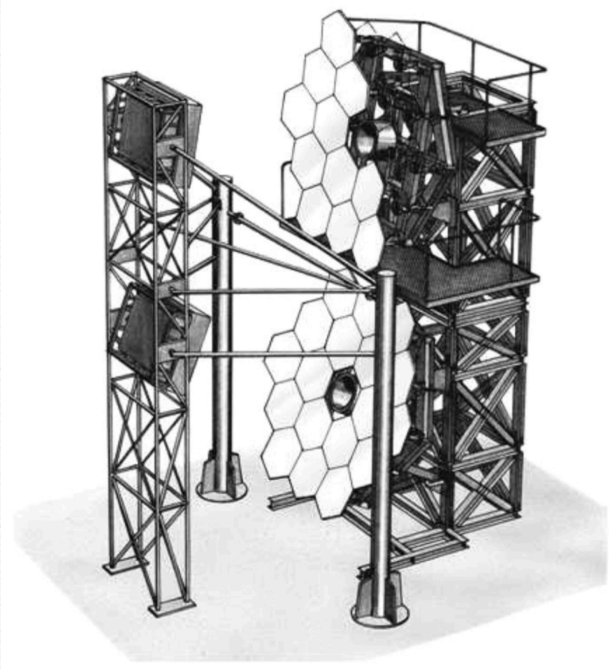

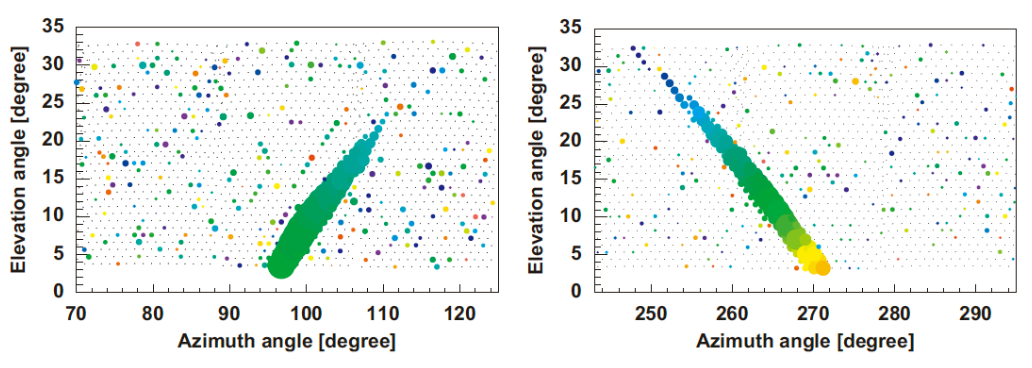

Telescope Array
SD

[tok11, abu12,]

700 km² (~30kmφ)

507 plastic scintillation counter of 3m²×1.2cm×2 layers

mean distance 1.2 km on square grid

~0.7 SD / km²

104 wavelength-shifting fibers

PMT 9124SA; Electron Tubes Ltd.

12bit 50 MHz FADC

Time recording calibrated by GPS.

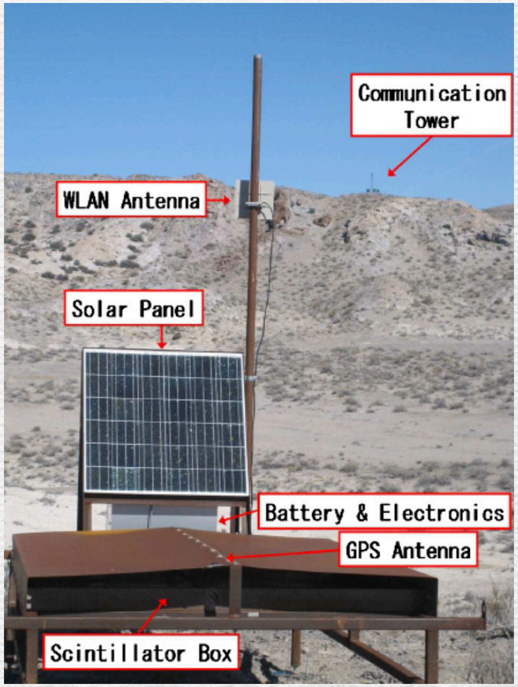

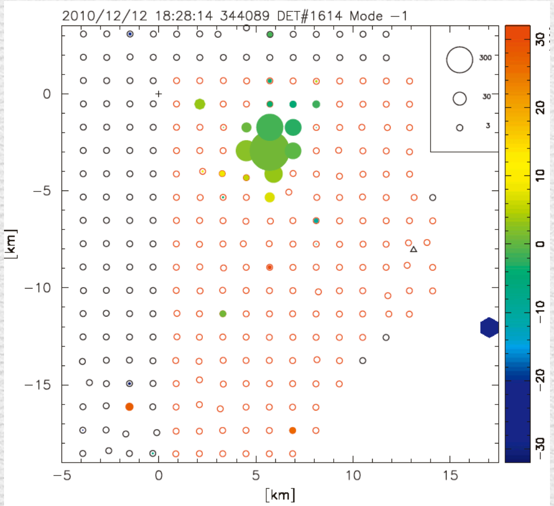

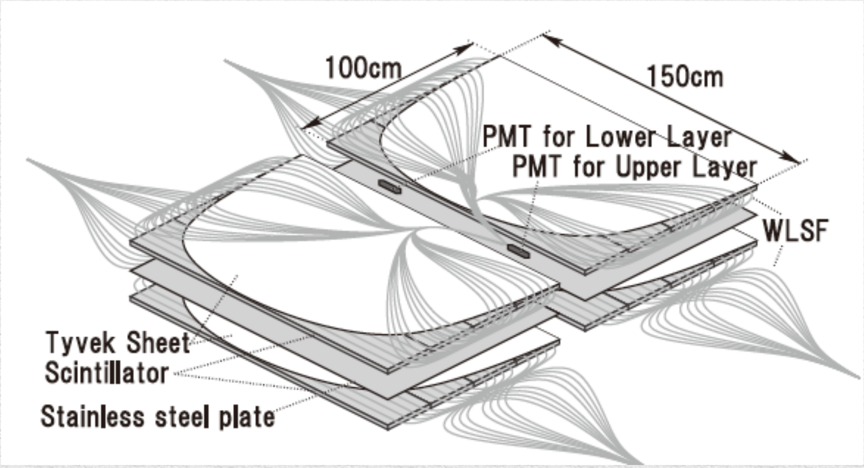

Analysis Methods

Analysis Methods
Event Reconstruction

[aug15]

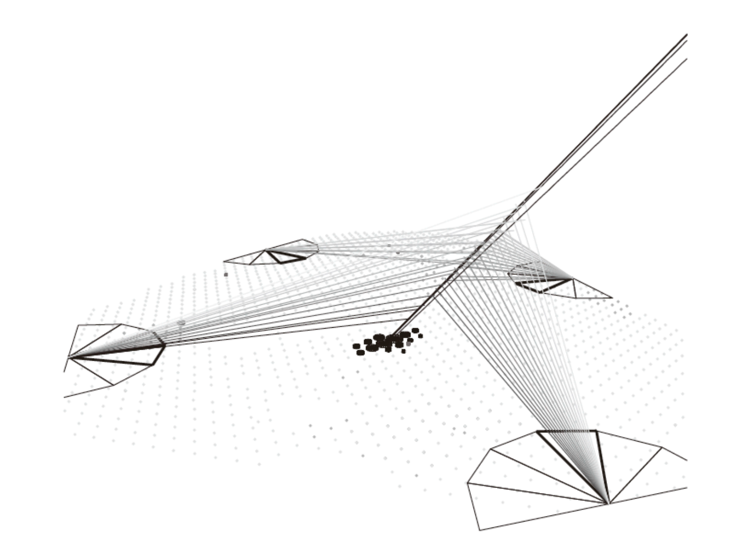

Fig. 33. Geometry reconstruction of an event observed by four telescopes and the surface detector.

Direction of CR: time difference of SD signals

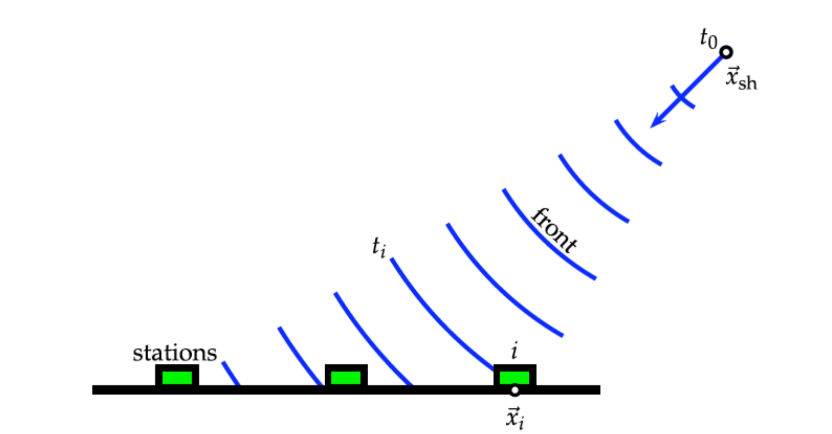

Fig. 35. Reconstruction of shower geometry: schematic representation of the evolution of the shower front.

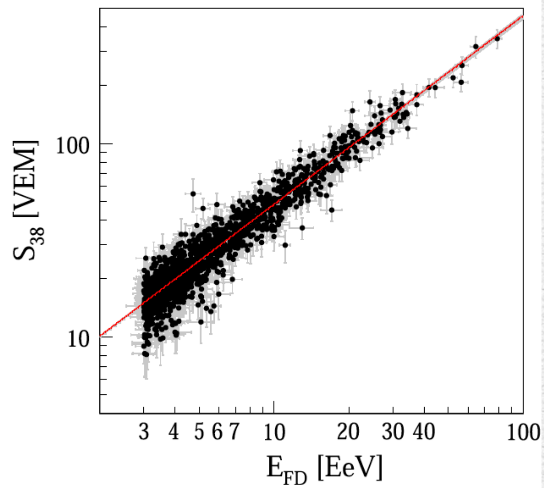

Fig. 41. Correlation between S_{38} and E_{FD} [11,122].

Absolute energy: sum of the FD signal
 with correction
  atmospheric attenuation
  escaped events (muon, neutrino) ~10%
systematic uncertainty: 14%

The signal size (θ=38°) of SD:
 correlated with CR energy, calibrated to FD.

VEM: Vertical Equivalent Muon

Analysis Methods
FD

[anc19]

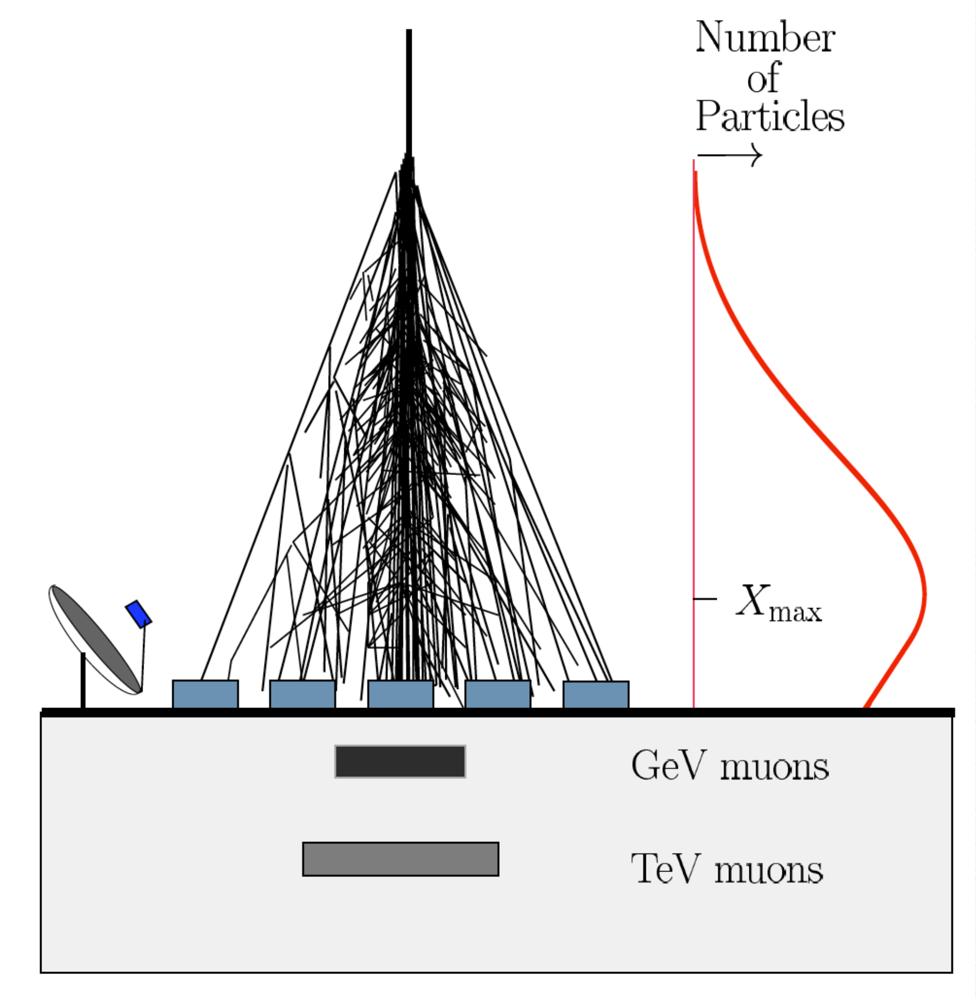

X_{max}:
atmospheric depth by FD data where the maximum number of particles is the largest.

$<X_{max}>$: mean of X_{max}

$\sigma(<X_{max}>)$: standard deviation of X_{max}

for the events of interest

$<X_{max}>$ and $\sigma(<X_{max}>)$ are predicted to be correlated with the mass (A) of the primary CR.

The correlation depends on the hadronic shower model.

Primary beam energy is above where accelerate laboratory data are available.

X_{max} distribution predictions

[aab14]

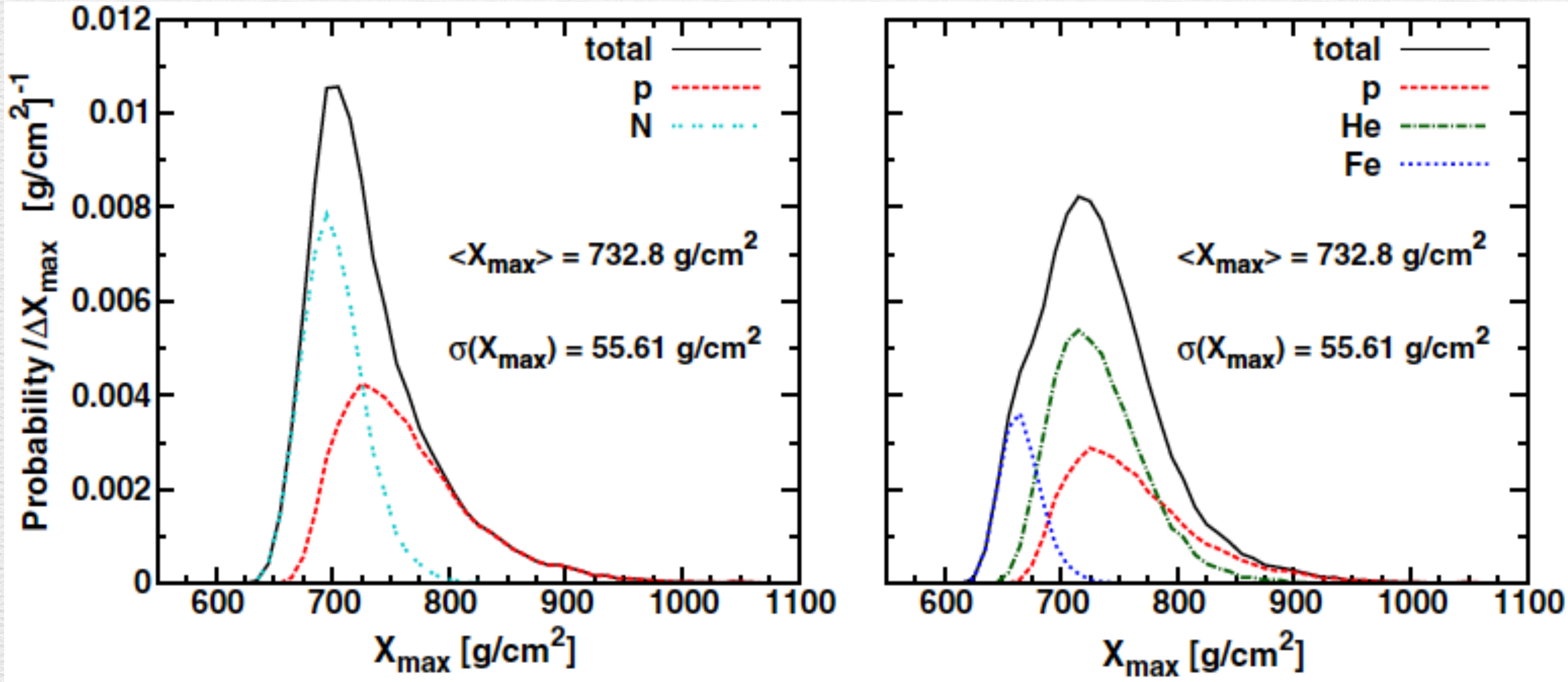

Composition

Mass Composition

[gor18]

Pierre Auger Observatory

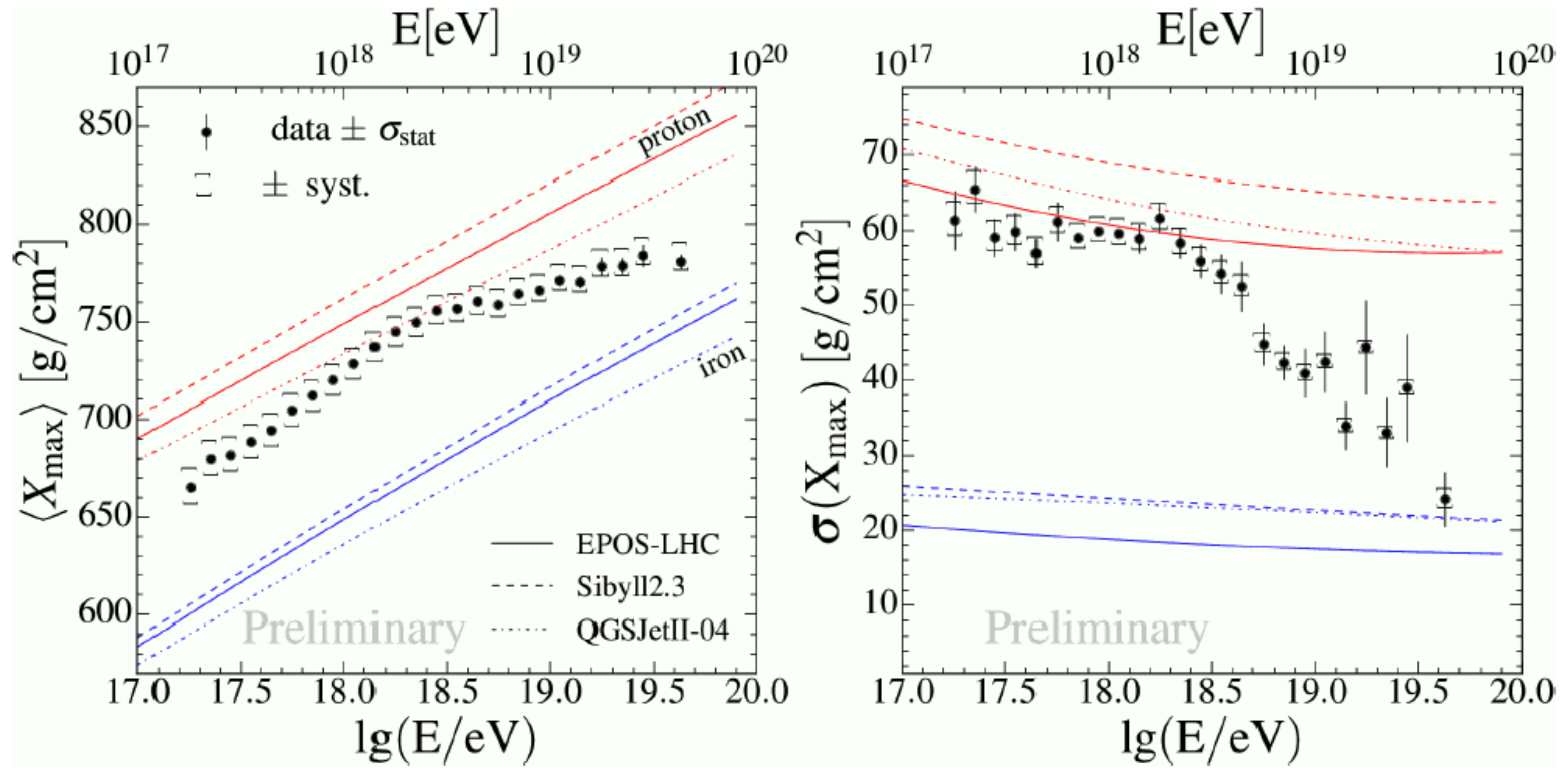

The fraction of proton increases up to $10^{18.3}$ eV and then decreases.

Composition of heavier mass nuclei are becoming dominating at the highest energy.

Ultra-High-Energy Cosmic Rays (UHECRs) [PDG2018]

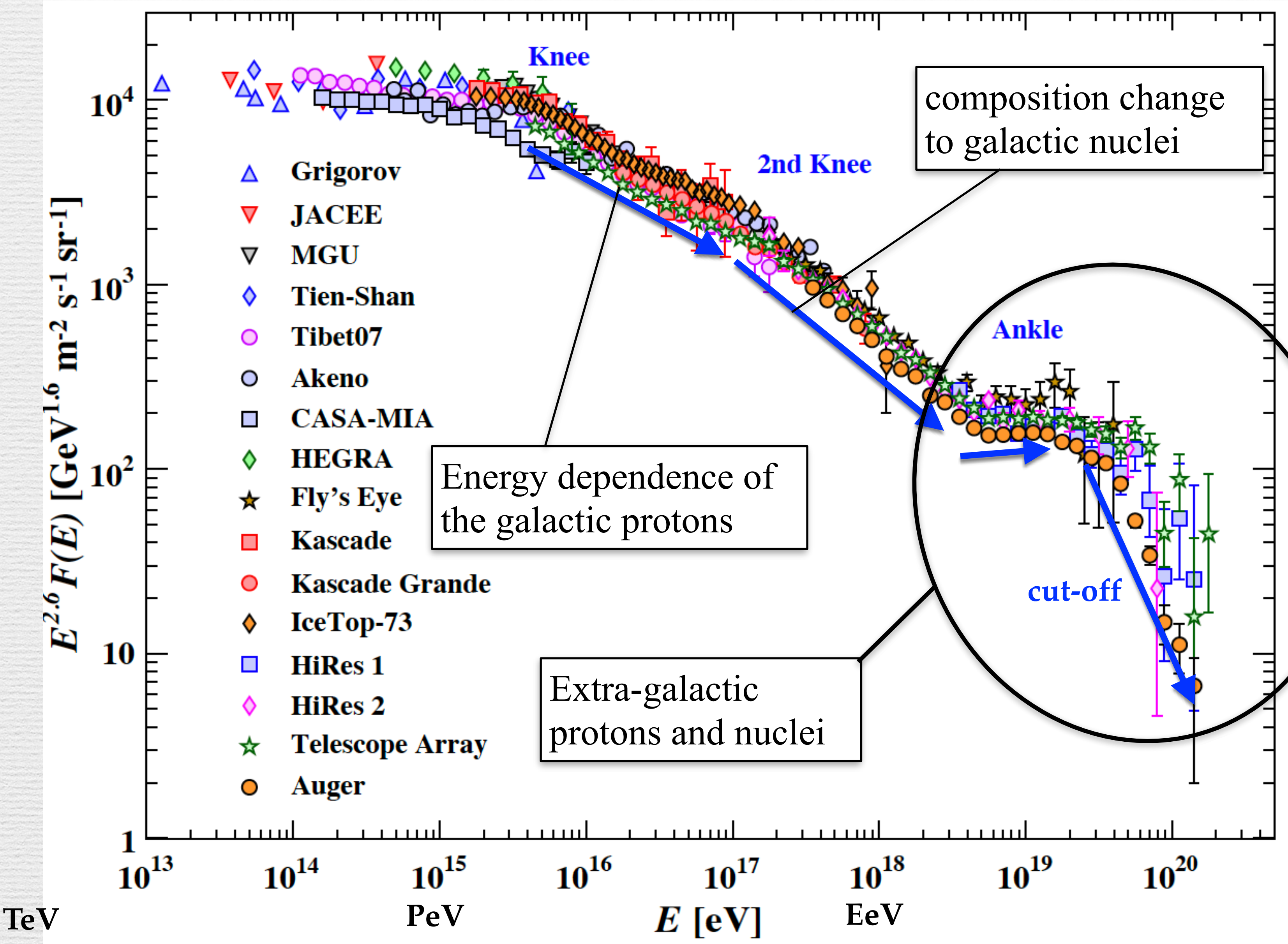

Anisotropy

Anisotropy

Pierre Auger Observatory

[aab18]

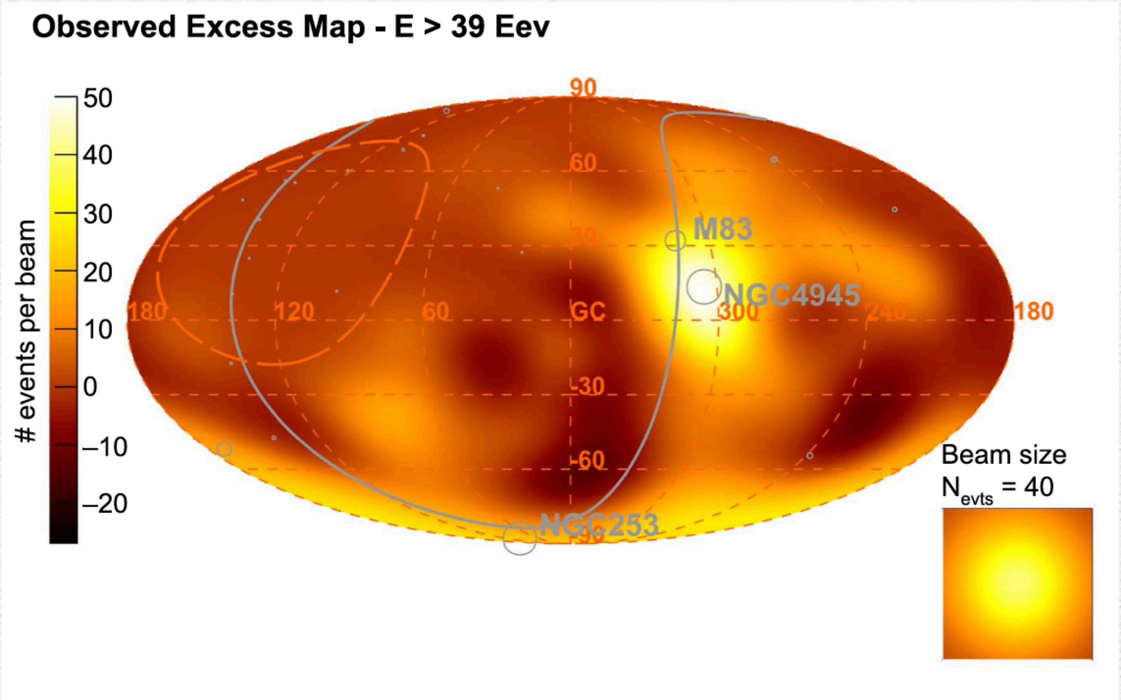

The observed anisotropy showed correlation with the distribution of SBGs (4.0σ).

SBG: star burst galaxy

γAGN: γ-active galactic nucleus

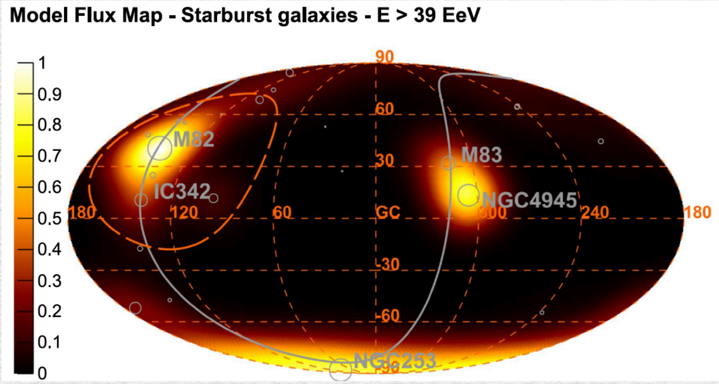

Prediction of UHECR intensity assuming SBGs as the source including attenuation in the extragalactic propagation.

Note that the region (surrounded by the dashed line) close to M82 is not covered by Auger.

Anisotropy

Pierre Auger Observatory

[aab18]

Table 1
Populations Investigated

SBGs	l (°)	b (°)	Distance[a] (Mpc)	Flux Weight (%)	Attenuated Weight: A/B/C (%)	% Contribution[b]: A/B/C (%)
NGC 253	97.4	−88	2.7	13.6	20.7/18.0/16.6	35.9/32.2/30.2
M82	141.4	40.6	3.6	18.6	24.0/22.3/21.4	0.2/0.1/0.1
NGC 4945	305.3	13.3	4	16	19.2/18.3/17.9	39.0/38.4/38.3
M83	314.6	32	4	6.3	7.6/7.2/7.1	13.1/12.9/12.9
IC 342	138.2	10.6	4	5.5	6.6/6.3/6.1	0.1/0.0/0.0
NGC 6946	95.7	11.7	5.9	3.4	3.2/3.3/3.5	0.1/0.1/0.1
NGC 2903	208.7	44.5	6.6	1.1	0.9/1.0/1.1	0.6/0.7/0.7
NGC 5055	106	74.3	7.8	0.9	0.7/0.8/0.9	0.2/0.2/0.2
NGC 3628	240.9	64.8	8.1	1.3	1.0/1.1/1.2	0.8/0.9/1.1
NGC 3627	242	64.4	8.1	1.1	0.8/0.9/1.1	0.7/0.8/0.9
NGC 4631	142.8	84.2	8.7	2.9	2.1/2.4/2.7	0.8/0.9/1.1
M51	104.9	68.6	10.3	3.6	2.3/2.8/3.3	0.3/0.4/0.5
NGC 891	140.4	−17.4	11	1.7	1.1/1.3/1.5	0.2/0.3/0.3
NGC 3556	148.3	56.3	11.4	0.7	0.4/0.6/0.6	0.0/0.0/0.0
NGC 660	141.6	−47.4	15	0.9	0.5/0.6/0.8	0.4/0.5/0.6
NGC 2146	135.7	24.9	16.3	2.6	1.3/1.7/2.0	0.0/0.0/0.0
NGC 3079	157.8	48.4	17.4	2.1	1.0/1.4/1.5	0.1/0.1/0.1
NGC 1068	172.1	−51.9	17.9	12.1	5.6/7.9/9.0	6.4/9.4/10.9
NGC 1365	238	−54.6	22.3	1.3	0.5/0.8/0.8	0.9/1.5/1.6
Arp 299	141.9	55.4	46	1.6	0.4/0.7/0.6	0.0/0.0/0.0
Arp 220	36.6	53	80	0.8	0.1/0.3/0.2	0.0/0.2/0.1
NGC 6240	20.7	27.3	105	1	0.1/0.3/0.1	0.1/0.3/0.1
Mkn 231	121.6	60.2	183	0.8	0.0/0.1/0.0	0.0/0.0/0.0
γAGNs						
Cen A Core	309.6	19.4	3.7	0.8	60.5/14.6/40.4	86.8/56.3/71.5
M87	283.7	74.5	18.5	1	15.3/7.1/29.5	9.7/12.1/23.1
NGC 1275	150.6	−13.3	76	2.2	6.6/6.1/7.5	0.7/1.6/1.0
IC 310	150.2	−13.7	83	1	2.3/2.4/2.6	0.3/0.6/0.3
3C 264	235.8	73	95	0.5	0.8/1.0/0.8	0.4/1.3/0.5
TXS 0149 + 710	127.9	9	96	0.5	0.7/0.9/0.7	0.0/0.0/0.0
Mkn 421	179.8	65	136	54	11.4/48.3/14.7	1.8/19.1/2.8
PKS 0229-581	280.2	−54.6	140	0.5	0.1/0.5/0.1	0.2/2.0/0.3
Mkn 501	63.6	38.9	148	20.8	2.3/15.0/3.6	0.3/5.2/0.6
1ES 2344 + 514	112.9	−9.9	195	3.3	0.0/1.0/0.1	0.0/0.0/0.0
Mkn 180	131.9	45.6	199	1.9	0.0/0.5/0.0	0.0/0.0/0.0
1ES 1959 + 650	98	17.7	209	6.8	0.0/1.7/0.1	0.0/0.0/0.0
AP Librae	340.7	27.6	213	1.7	0.0/0.4/0.0	0.0/1.3/0.0
TXS 0210 + 515	135.8	−9	218	0.9	0.0/0.2/0.0	0.0/0.0/0.0
GB6 J0601 + 5315	160	14.6	232	0.4	0.0/0.1/0.0	0.0/0.0/0.0
PKS 0625-35	243.4	−20	245	1.3	0.0/0.1/0.0	0.0/0.5/0.0
I Zw 187	77.1	33.5	247	2.3	0.0/0.2/0.0	0.0/0.0/0.0

Studying the correlation between the UHECR anisotropy and the distribution of galaxies from the 2FHL catalog (FERMI-LAT)

SBG: star burst galaxy

γAGN: γ-active galactic nucleus

Energy Loss Process in Space Propagation

Greisen, Zatzepin, and Kuzmin (GZK) Cut-off

[gre66,zat66]

GZK predicted a cutoff of UHECR flux at around 10^{20} eV
due to energy-loss with the collision of CMB in extragalactic propagation

For UHECR nuclei

photo-absorption of CMB

→ excitation to GDR

→ disintegration (photo-disintegration)

Cosmic Microwave Background (CMB)

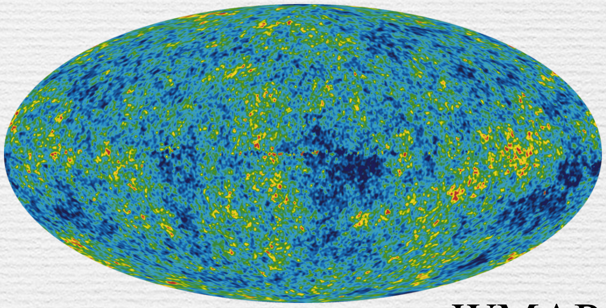

WMAP

T=2.72548±0.00057 K

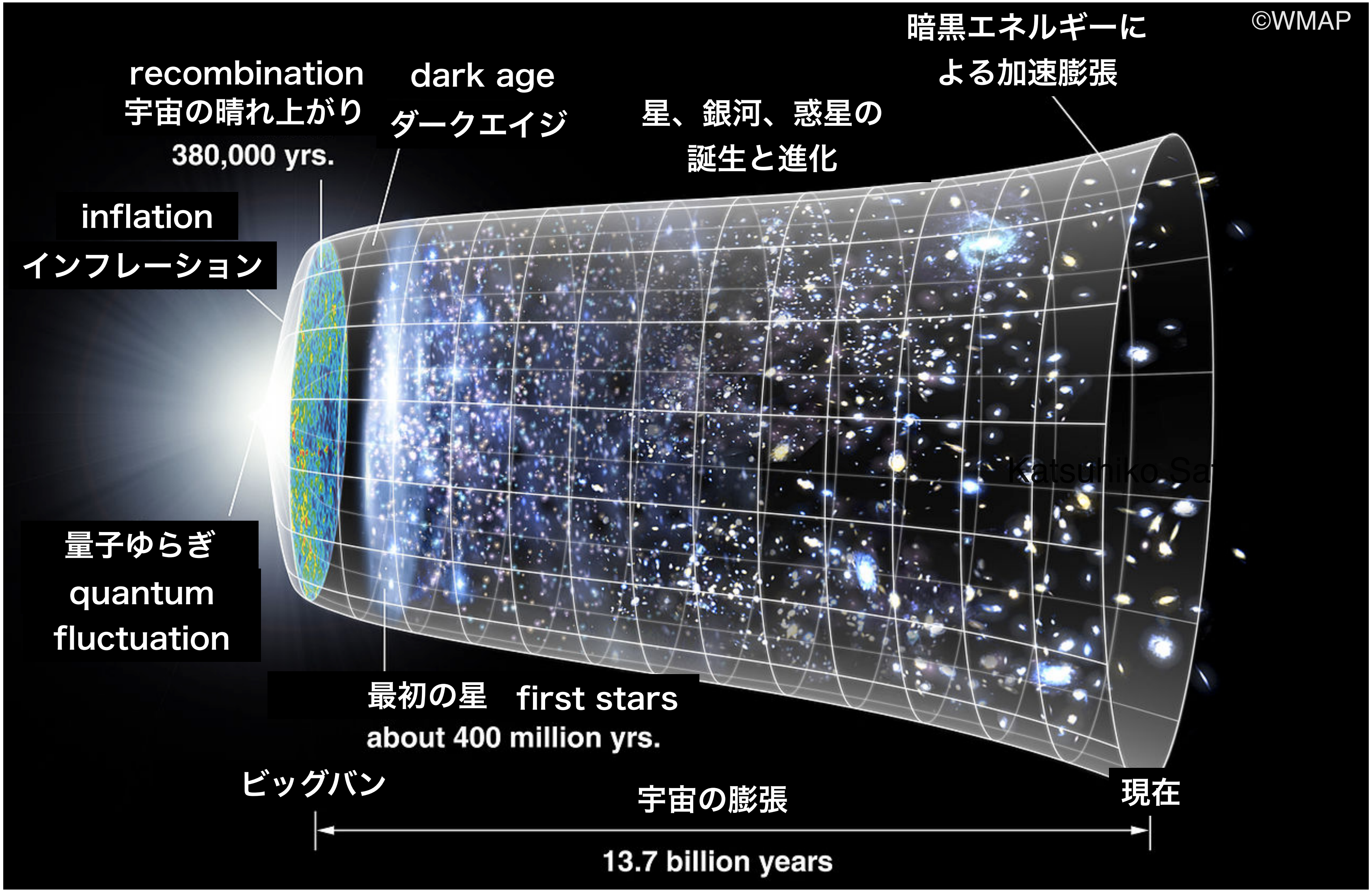
©WMAP
暗黒エネルギーに
よる加速膨張
recombination
宇宙の晴れ上がり
380,000 yrs.
dark age
ダークエイジ
星、銀河、惑星の
誕生と進化
inflation
インフレーション
量子ゆらぎ
quantum
fluctuation
Katsuhiko Sa
最初の星 first stars
about 400 million yrs.
ビッグバン
宇宙の膨張
現在
13.7 billion years

in 1940's

"The elements in the universe must have been produced in a hot temperature that existed in the beginning of universe."

Gorge Gamow

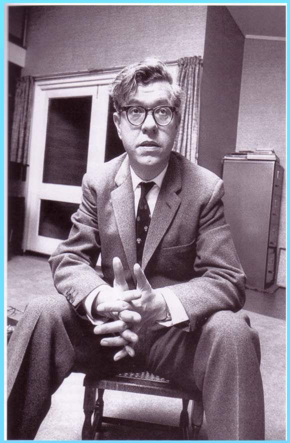

"What a stupid idea that the universe was in a Big Bang…"

Fred Hoyle

Discovery of the Cosmic Microwave Background (CMD)

A direct evidence of the existence of Big Bang.

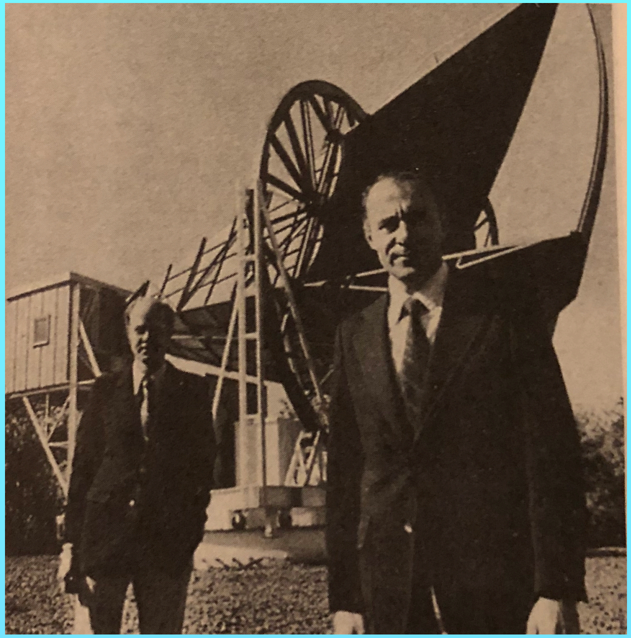

1964-65
Arno A. Penzias (right)
Robert R. Wilson (left)

There exists a noise coming from any direction that can never be eliminated.

High-sensitivity antenna

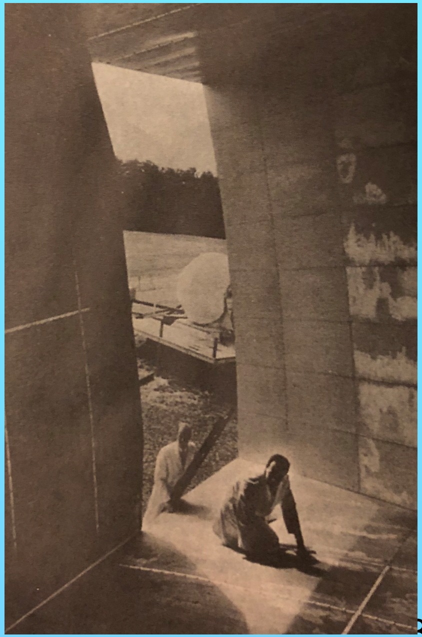

Satellite Observation:
COBE(1989-96), WMAP(2001-), PLANCK(2009-)

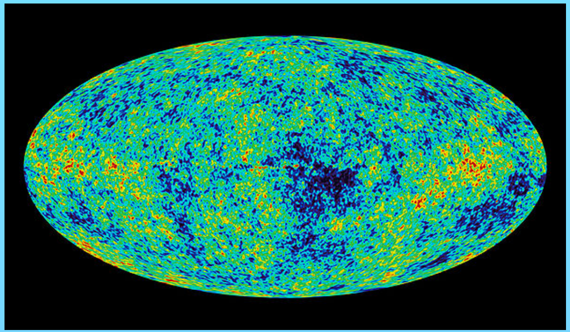

WMAP

T=2.72548±0.00057 K

Greisen, Zatzepin, and Kuzmin (GZK) Cut-off

[gre66,zat66]

GZK predicted a cutoff of UHECR flux at around 10^{20} eV
due to energy-loss with the collision of CMB in extragalactic propagation

For UHECR protons
pion production by photo-proton interaction

For UHECR nuclei
photo-absorption of CMB
→ excitation to GDR
→ disintegration (photo-disintegration)

Cosmic Microwave Background (CMB)

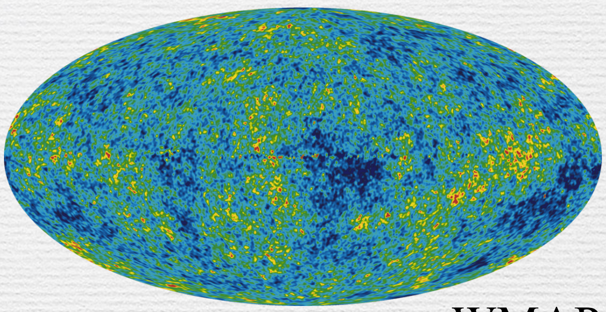

WMAP

T=2.72548±0.00057 K

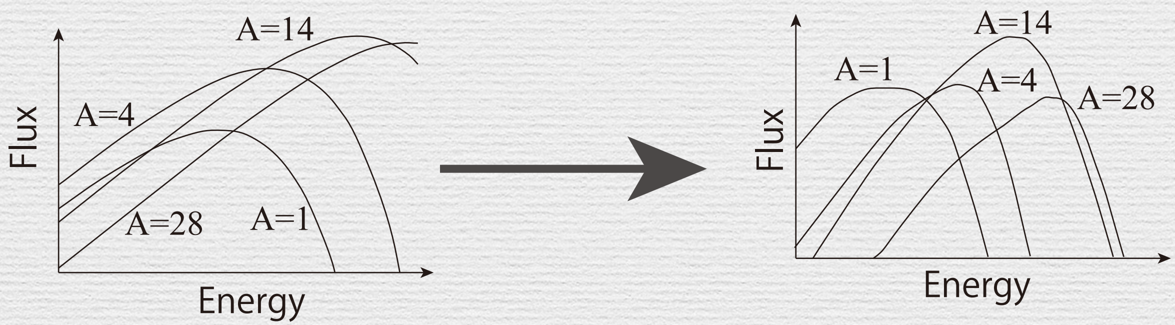

Production at Extra Galaxies

Observation on Earth

Greisen, Zatzepin, and Kuzmin (GZK) Cut-off

[gre66,zat66]

GZK predicted a cutoff of UHECR flux at around 10^{20} eV
due to energy-loss with the collision of CMB in extragalactic propagation

For UHECR nuclei

photo-absorption of CMB

→ excitation to GDR

→ disintegration (photo-disintegration)

Cosmic Microwave Background (CMB)

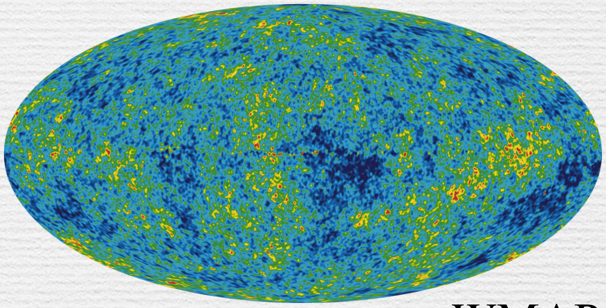

WMAP

T=2.72548±0.00057 K

Photo-nuclear reactions determine the travel distance of UHECRs nuclei and their composition/energy modification in extra-galactic propagation.

PANDORA

Photo-Absorption of Nuclei and Decay Observation for Reactions in Astrophysics

PANDORA Project

Photo-**A**bsorption of **N**uclei and **D**ecay **O**bservation for **R**eaction in **A**strophysics

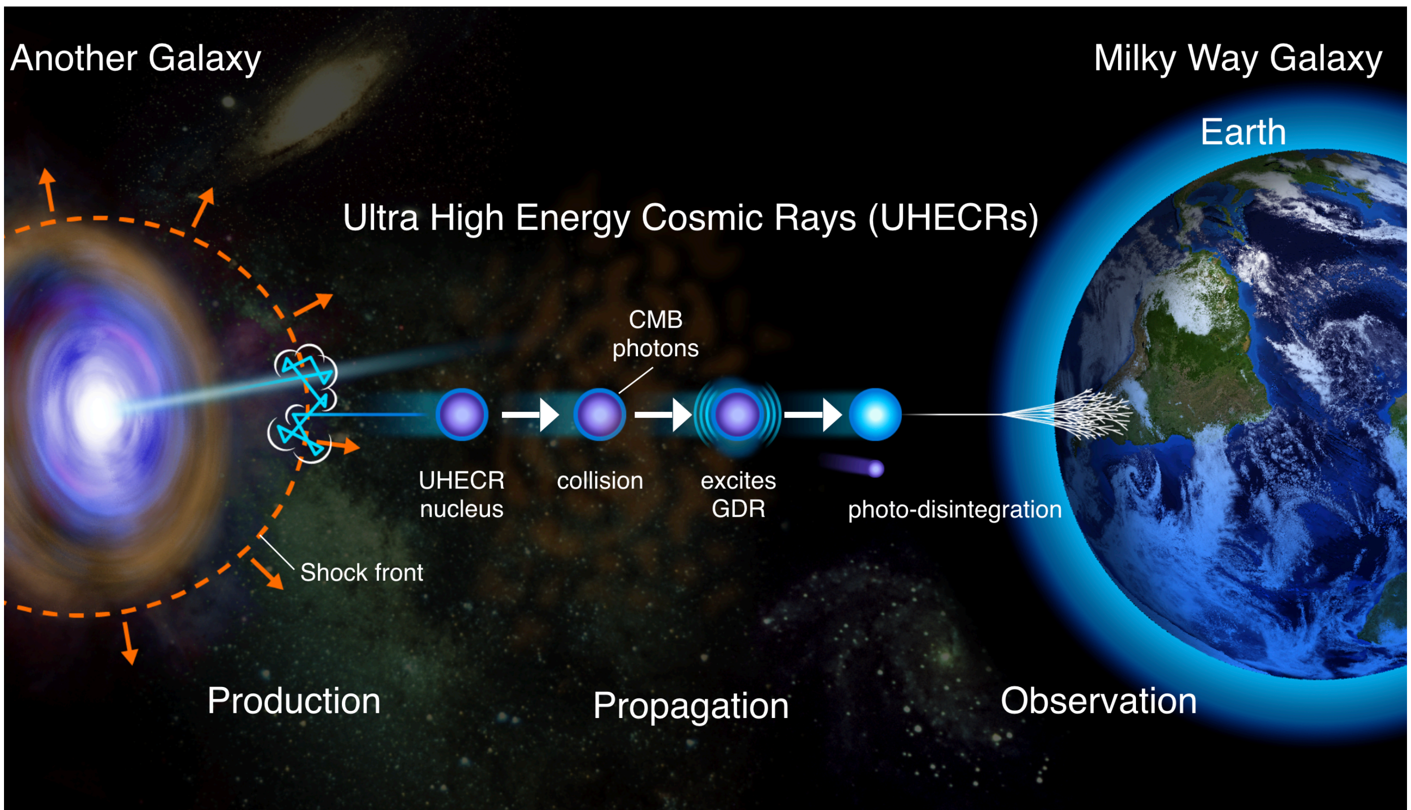

Systematic Measurement on E1 Strength Distribution and n,p,α,γ decays up to A~60

- E1 excitation strength distribution
- n, p, α, γ decay branching ratios
- from light to A~60 for stable nuclei

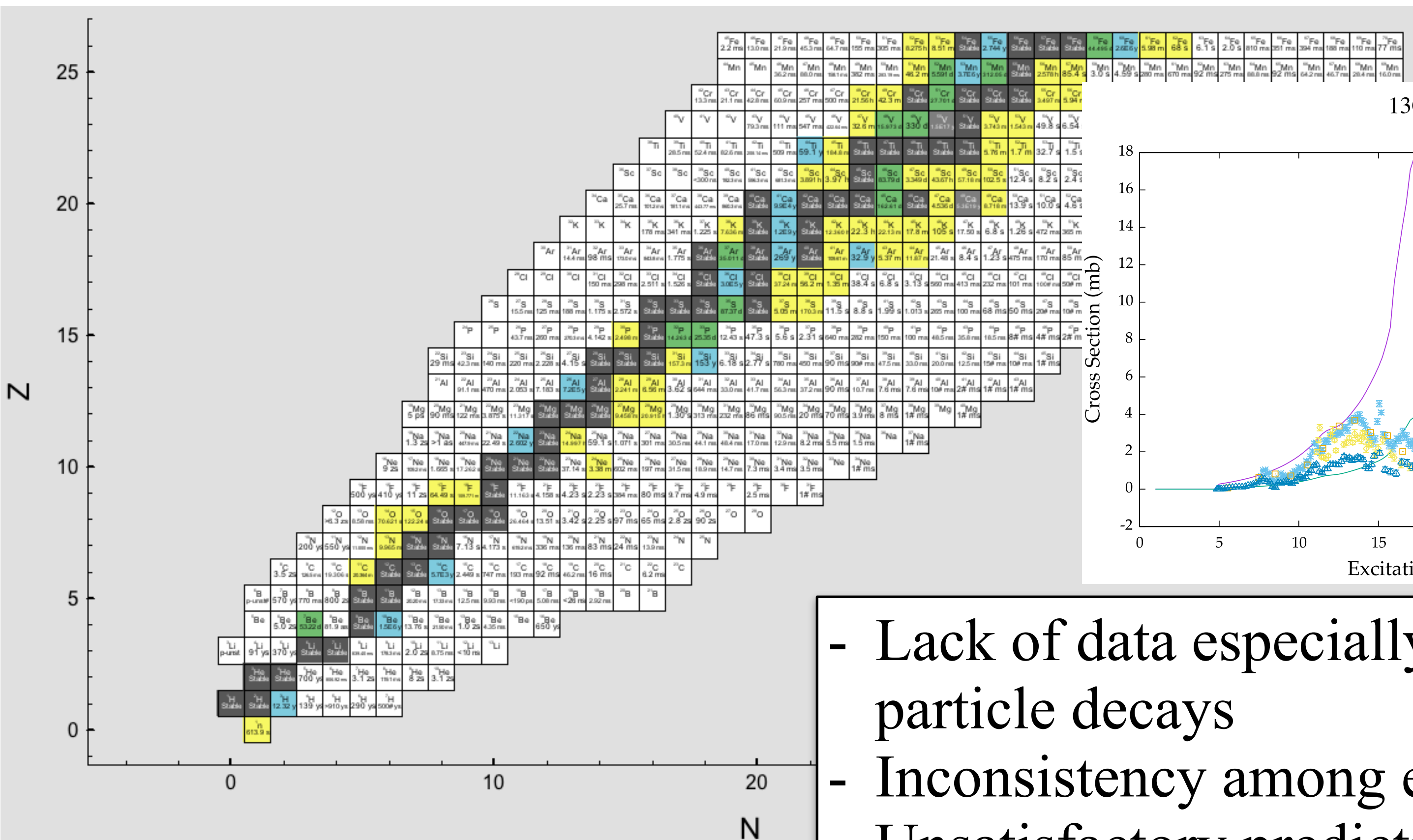

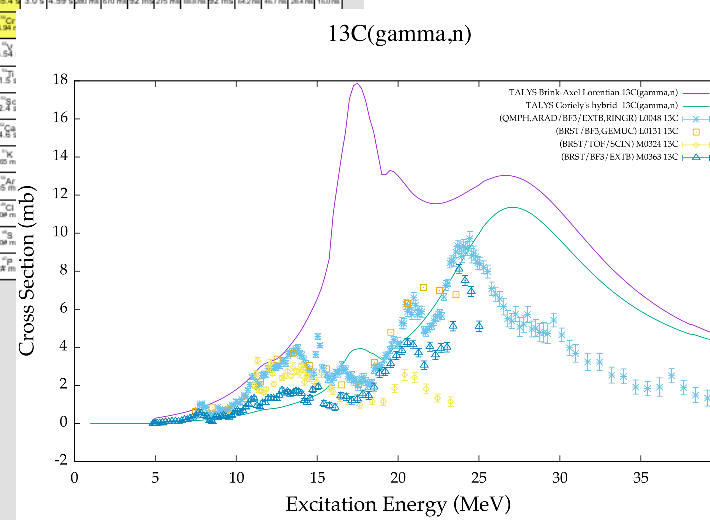

- Lack of data especially for charged particle decays
- Inconsistency among experiments
- Unsatisfactory prediction by models

Photo-Nuclear Reactions of Light Nuclei

Astro-nuclear Physics, Astro-particle Physics

Energy-loss process of UHCRs

Nucleosynthesis

Neutral current neutrino detection: gamma-emission of GRs

Radiation shield, decommissioning, reactions in nuclear reactors

Photo-radiation Analysis, nondestructive inspection

γ-imaging、CT-Diagnostics、Biological Effects

Home-Land Security、Inspection of fission or explosive material

Medical RI production by photo-irradiation

Nuclear reaction/gamma radiation in thunder volts

99.99999% of the elements consists of nuclei below A=60

Photo-Nuclear Reaction

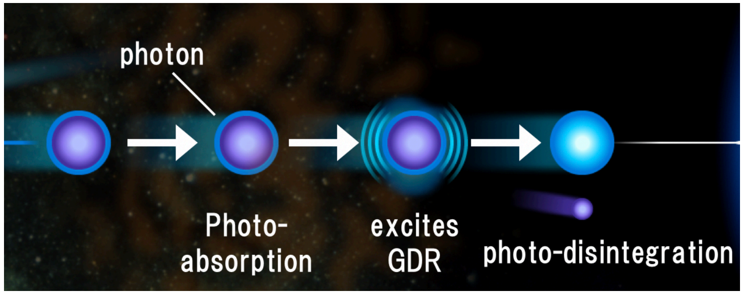

GDR:Giant Dipole Resonance

is ”described” as
photo-absorption process + decay process

Nuclear excitation by photo-absorption ≃ electric dipole excitation of nuclei

$$\sigma_{\text{abs}} = \frac{16\pi^3}{9}\alpha E \frac{dB(E1)}{dE}$$

σ_{abs} : photo-absorption cross section

$B(E1)$: electric-dipole reduced transition probability of the nucleus

E : photon-energy = nuclear excitation energy

Is the photo-absorption cross section well understood?

Is the photo-absorption cross section well understood?

Being studied since the discovery of GDR

However, systematic studies are limited in heavy nuclei for (γ,xn) processes

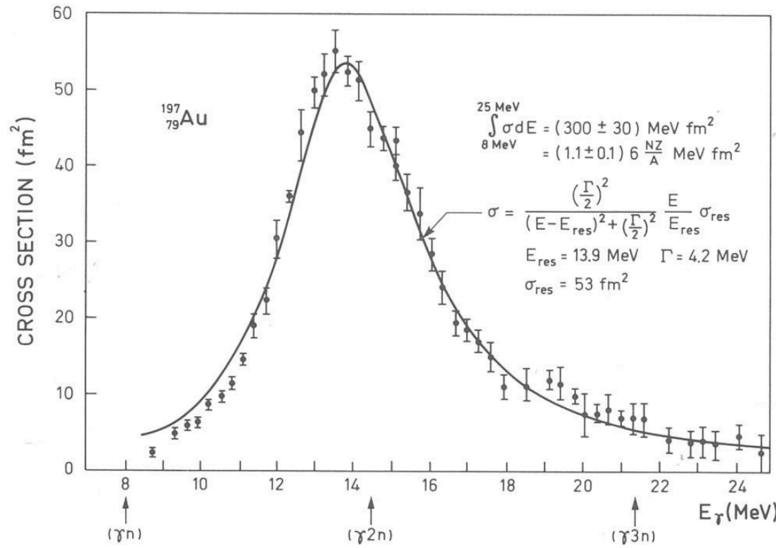

Comparison with the TRK sum rule

up to 30 MeV

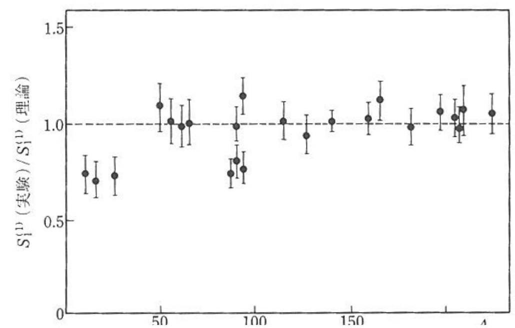

up to 140 MeV

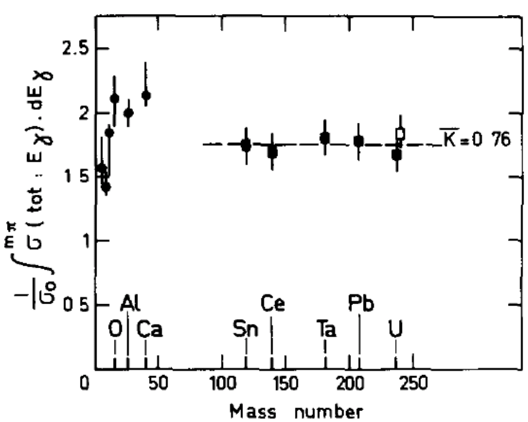

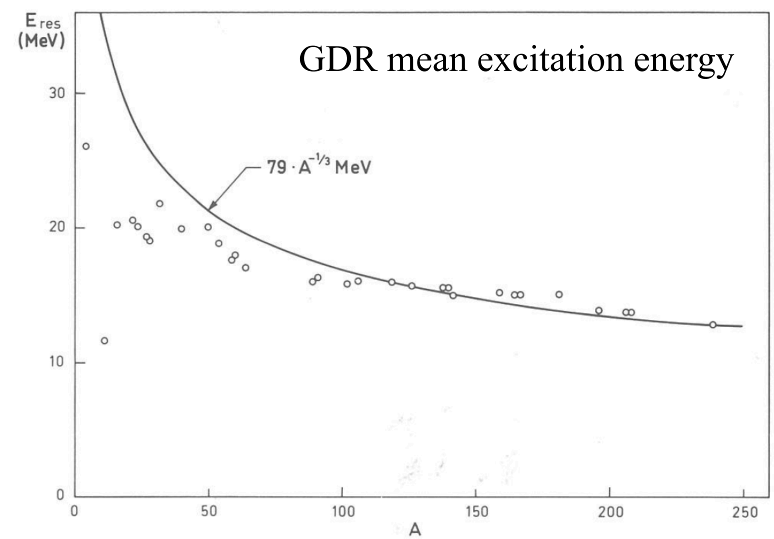

Bohr and Mottelson

Is the photo-absorption cross section well understood?

For light nuclei

- photo-abs. c.s. $\neq$ (γ,xn) c.s.

large branch to *p* and α emissions

- More complicated description is required for theoretical models

Structure

- stronger shell effect
- nuclear deformation
- nucleon correlations:

α clustering, *np* pairing, tensor correlation

Decay

- pre-equilibrium decay process
- isospin selection rule in the α-decay process

^{13}C(γ,n)

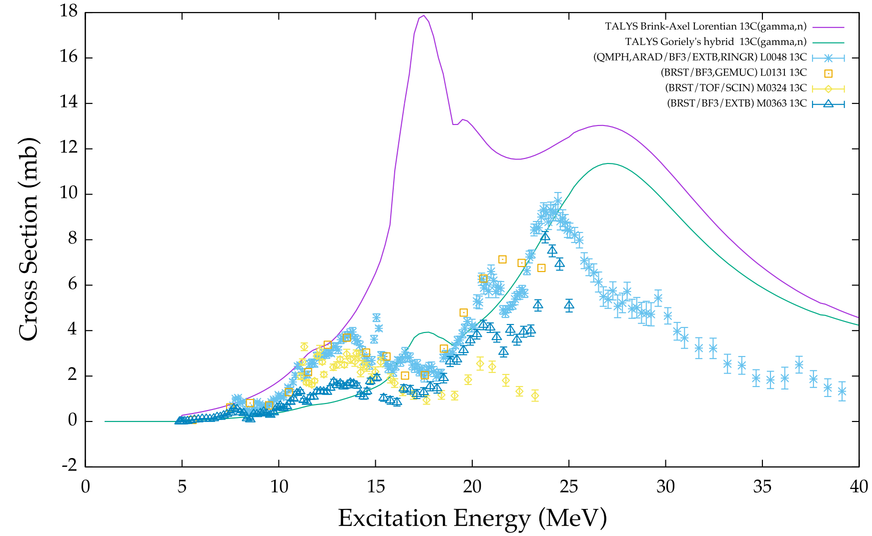

Example: ^{13}C(γ,xn) reaction data and predictions

- Lack of data especially for charged particle decays
- Large inconsistency among experimental data
- Unsatisfactory theoretical predications

$$^{12}\mathrm{C}(T=0)+\gamma \rightarrow \ ^{12}\mathrm{C}^*(\mathrm{GDR}:T=1)$$

$$\not\rightarrow \ ^{8}\mathrm{Be}(T=0)+\alpha(T=0)$$

isospin forbidden

Is the photo-absorption cross section well understood?

For light and medium mass nuclei

- photo-abs. c.s. $\neq$ (γ,xn) c.s.

significant contribution from *p* and α emission channels

- More complicated description is required for theoretical models

Structure

- stronger shell effect
- nuclear deformation
- nucleon correlations:

  α clustering, *np* pairing, tensor correlation,…

Decay

- pre-equilibrium decay process
- isospin selection rule in the decay process

Ahrens et al. (γ,abs)

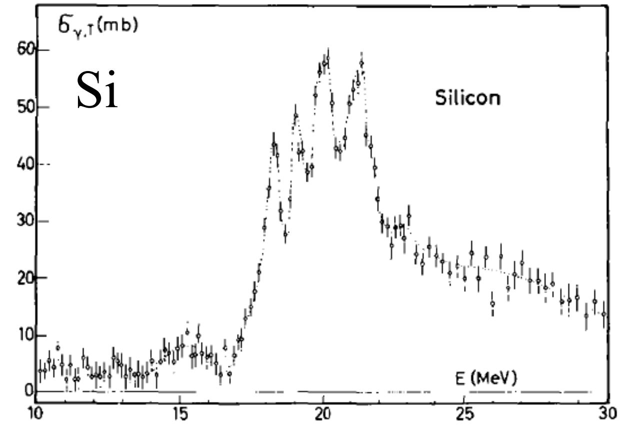

Harada et al. γ-transmission

Matsubara et al., (p,p')

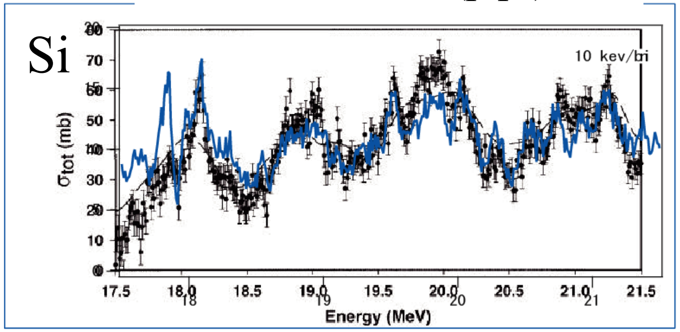

Why are the available data so inaccurate?

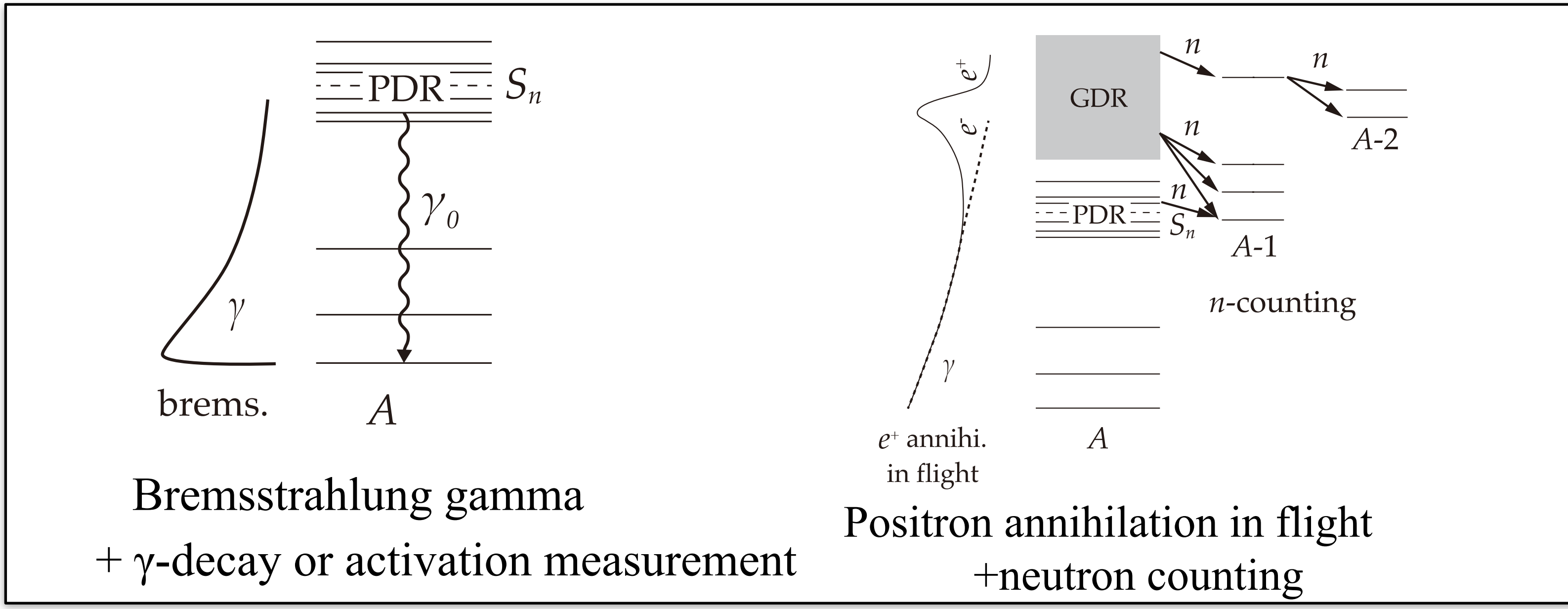

historical methods

A. Bracco, E.G. Lanza, AT, PPNP **106**, 360 (2019)

- **continuous energy spectrum** of Bremsstrahlung gamma-rays

  large systematic uncertainty to taking **difference with changing the electron beam energy**

  gamma-decay measurement only detects transitions to the ground state

- positron annihilation in flight

  needs to take **difference between e+ and e-** for cancelling atomic process gamma-rays

  flat *n* detection efficiency in energy **is assumed** in the neutron counting

- charged particle decay measurement is difficult due to **low gamma intensity** and **thick target**
- **bad energy resolution** ≳ 500 keV

Modern Experimental Methods

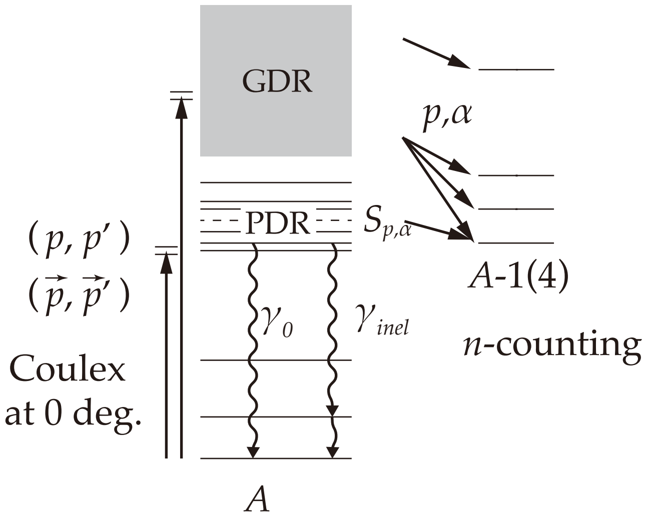

virtual phon excitation by proton
& decay coincidence

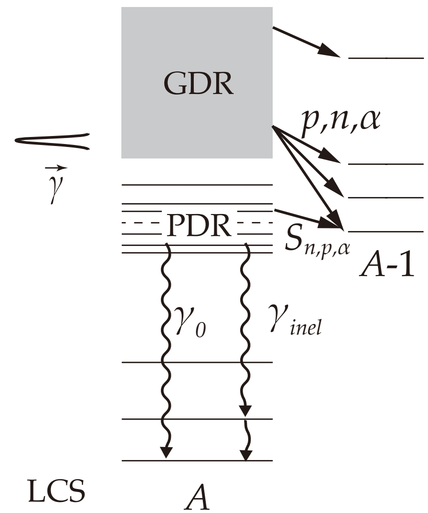

quasi-mono-energy gamma by LCS
& decay coincidence

A. Bracco, E.G. Lanza, AT, PPNP **106**, 360 (2019)

- **virtual photon excitation** (proton Coulex) at RCNP and iThemba LABS

  Tag of excitation energy by scattered proton. Sensitive to **total photo-absorption c.s.**

  Good energy resolution of ~30 keV

  distribution

  C.S. is large, applicable to **isotopically enriched target** and **charged particle decays.**
  Spin-M1 and SDR are observed simultaneously.

  absolute c.s.

- **real photon excitation** by LCS gamma at ELI-NP

  high-intensity, applicable to **isotopically enriched target** and **charged particle decays**

  Good energy resolution of ~50 keV by **quasi-mono-energetic** LCS beam

  Precise absolute c.s. and **n decay**

Photo-Nuclear Reactions of Light Nuclei

What we wan to do

Prediction of photo-nuclear reactions from very light to Fe-Ni nuclei

What are the problems?

Data are very scarce, especially for charged particle decays

Serious inconsistencies among the existing data.

There are no “good” predictions by theoretical models
(developments in AMD, Shell-Model, RPA, Ab-Initio,…)

Decay process is not described well by theoretical models.

Direct and pre equilibrium decays are also important.

Statistical decay calculations are inacurate to light nuclei

Photo-disintegration Pass of ^{56}Fe

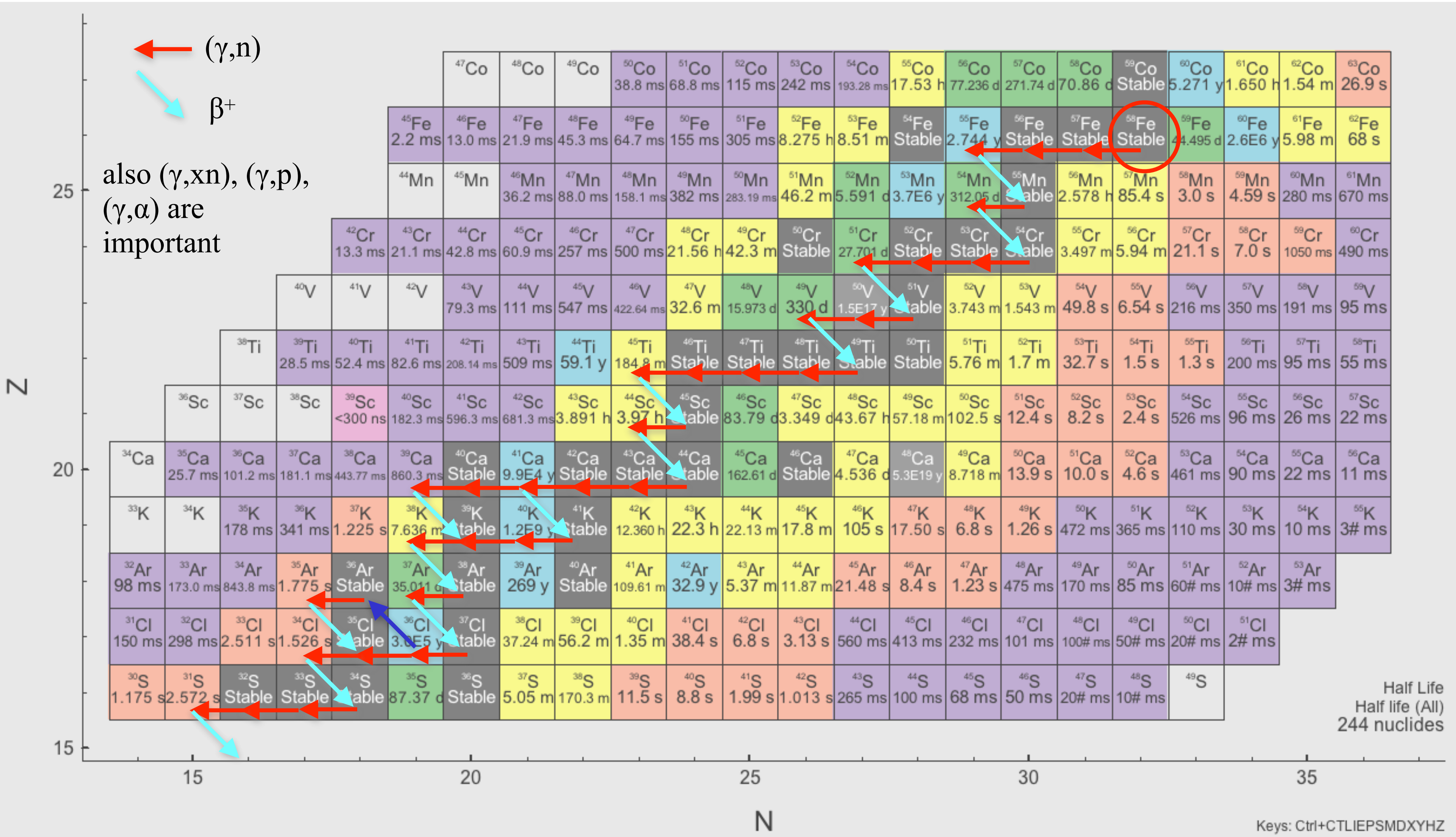

Photo-disintegration Pass of ^{56}Fe

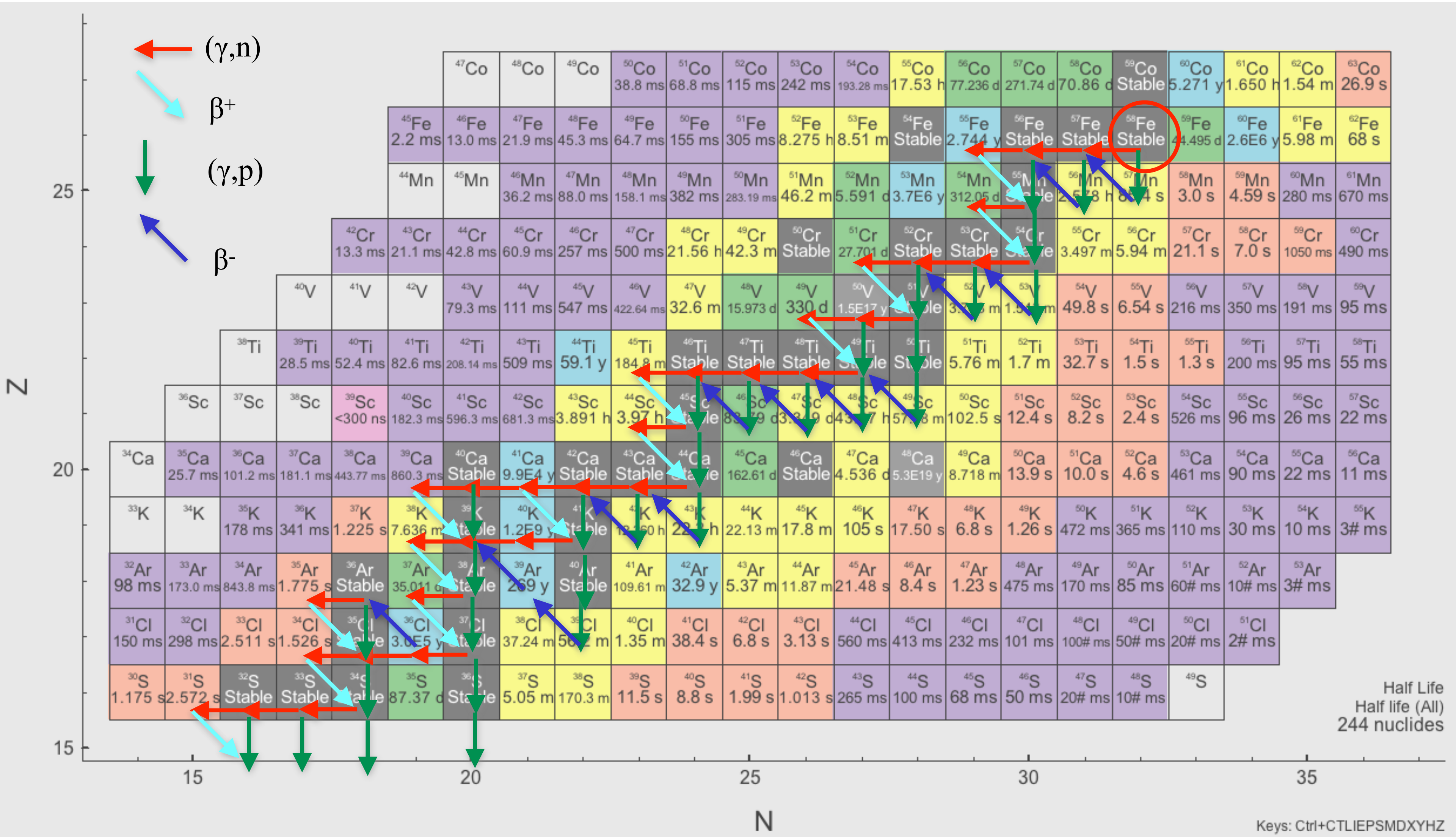

Also (γ,xn), (γ,α) are important

Unstable nuclei are also relevant up to $T_{1/2}$~1 min

Photo-disintegration Pass of ^{56}Fe

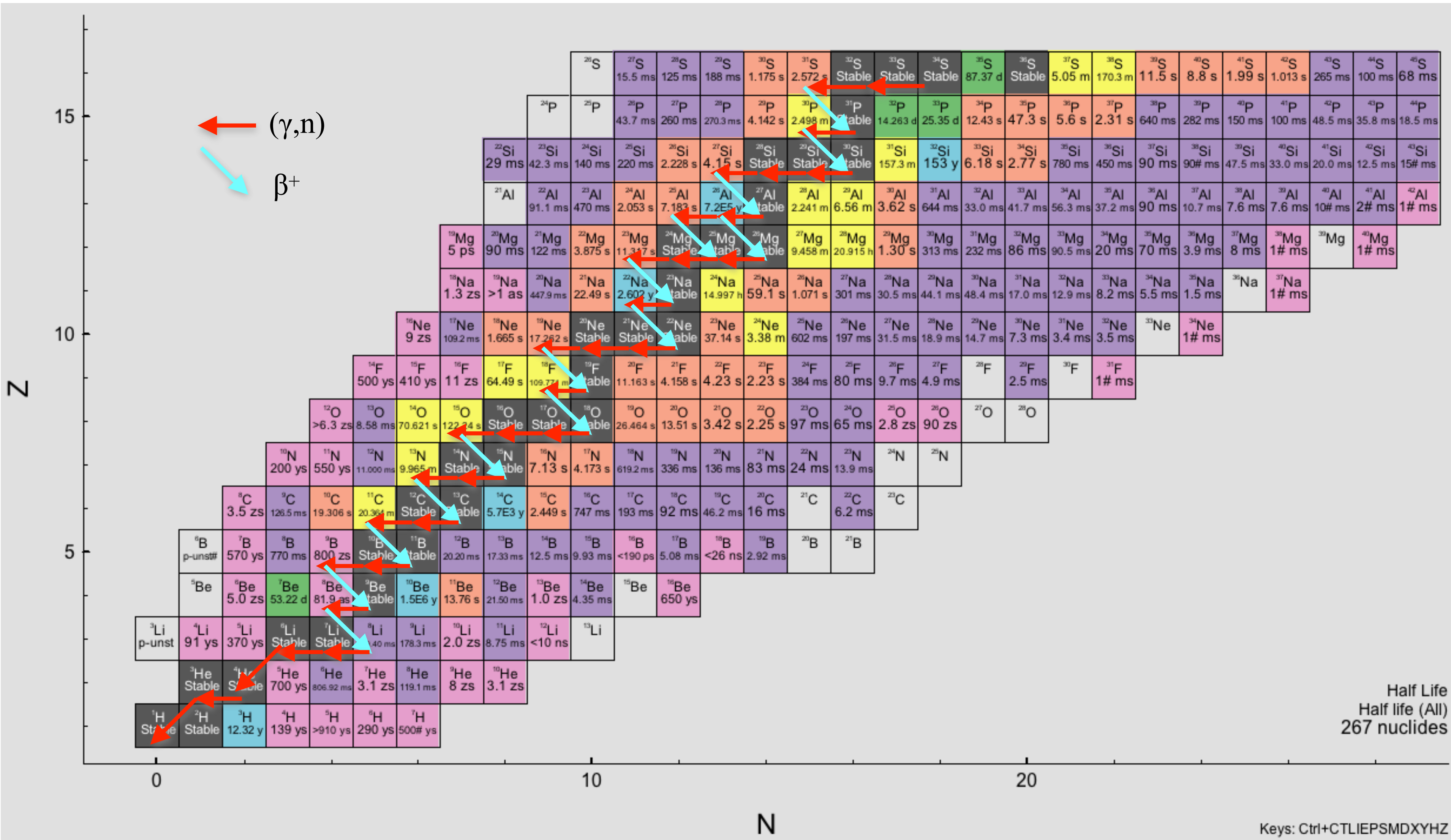

PANDORA Project: Collaboration

Nuclear Experiments

RCNP — *Osaka Univ.*
A. Tamii, N. Kobayashi, T. Sudo, M. Murata, A. Inoue, **R. Niina**, T. Kawabata, T. Furuno, S. Adachi, K. Sakanashi, K. Inaba, Y. Fujikawa, S. Okamoto, Y. Fujita, H. Fujita

ELI-NP — *ELI-NP*
P.-A. Söderström, D. Balabanski, L. Capponi, A. Dhal, T. Petruse, D. Nichita, Y. Xu

iThemba LABS — *iThemba LABS, Univ. Witwatersland, Stellenbosh Univ.*
L. Pellegri, R. Neveling, F.D. Smit, **J.A.C. Bekker**, S. Binda, H, Jivan, T. Khumal, M. Wiedeking, P. Adsley, L.M. Donaldson, E. Sideras-Haddado, K.L. Malatji, S. Jongile, A. Netshiya

TU-Darmstadt — P. von Neumann-Cosel, N. Pietralla, J. Isaak, J. Kleemann, M. Spall

U. Milano/INFN — A. Bracco, F. Camera, F. Crespi, O. Wieland

Shanghai — H. Utsunomiya

U. Oslo — K.C.W. Li, S. Siem, …

SLEGS | HIgS | NEPTUN | ELPH

Nuclear Theory

AMD — **M. Kimura, Y. Taniguchi**, H. Motoki

NRFT — **E. Litvinova**, P. Ring, H. Wibowo

RPA/DFT — RPA by **T. Inakura,** QPM by **N. Tsoneva**

Large Scale Shell Model — Y. Utsuno, N. Shimizu

TALYS — **S. Goriely, E. Khan**

PANDORA white paper published in EPJA (2023)

UHECR Theory

Propagation and production

D. Allard, B. Baret, I. Deloncle, J. Kiener, E. Parizot, V. Tatischeff

S. Nagataki, E. Kido, J. Oliver, H. Haoning

PANDORA Project: White Paper

PANDORA Project for the study of photonuclear reactions below A = 60

PANDORA Collaboration Euro. Phys. J. A **59**, 208 (2023)

A. Tamii[1,2,3,a], L. Pellegri[4,5], P.-A. Söderström[6], D. Allard[7], S. Goriely[8], T. Inakura[9], E. Khan[10], E. Kido[11], M. Kimura[11,12,13], E. Litvinova[14], S. Nagataki[11], P. von Neumann-Cosel[15], N. Pietralla[15], N. Shimizu[16], N. Tsoneva[6], Y. Utsuno[17], S. Adachi[18], P. Adsley[19,20], A. Bahini[5], D. Balabanski[6], B. Baret[7], J. A. C. Bekker[4,5], S. D. Binda[4,5], E. Boicu[6,21], A. Bracco[22,23], I. Brandherm[15], M. Brezeanu[6,21], J. W. Brummer[5], F. Camera[22,23], F. C. L. Crespi[22,23], R. Dalal[24], L. M. Donaldson[5], Y. Fujikawa[25], T. Furuno[3], H. Haoning[14], R. Higuchi[11], Y. Honda[3], A. Gavrilescu[6,26], A. Inoue[1], J. Isaak[15], H. Jivan[4,5], P. Jones[5], S. Jongile[5], O. Just[11,27], T. Kawabata[3], T. Khumalo[4,5], J. Kiener[10], J. Kleemann[15], N. Kobayashi[1], Y. Koshio[28], A. Kuşoğlu[6,29], K. C. W. Li[30], K. L. Malatji[5], R. E. Molaeng[4,5], H. Motoki[12], M. Murata[1], A. A. Netshiya[4,5,31], R. Neveling[5], R. Niina[1], S. Okamoto[25], S. Ota[1], O. Papst[15], E. Parizot[10], T. Petruse[6], M. S. Reen[32], P. Ring[33], K. Sakanashi[3], E. Sideras-Haddad[4], S. Siem[30], M. Spall[15], T. Suda[34], T. Sudo[1], Y. Taniguchi[35], V. Tatischeff[10], H. Utsunomiya[36,37], H. Wang[36,38,39], V. Werner[15], H. Wibowo[40], M. Wiedeking[4,5], O. Wieland[23], Y. Xu[6], Z. H. Yang[41]

A part of the visiting collaborators of RCNP-E563, Sep.-Oct., 2023

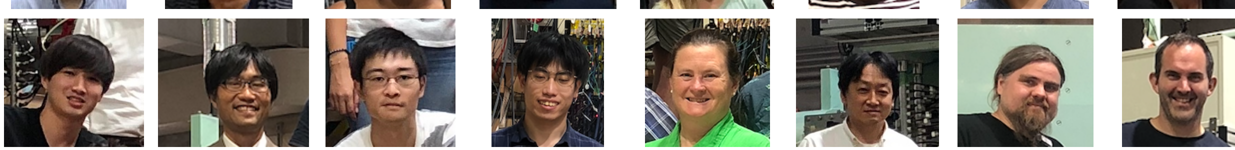

Thank you for your attention

2nd Proposal Submitted to RCNP

Photo-nuclear reactions of ^{16}O, ^{26}Mg, ^{40}Ca and ^{56}Fe (PANDORA project)

Spokespersons: A. Tamii, L. Pellegri P.-A. Söderström

EXPERIMENTAL GROUP:

F. Endo	RCNP
F. Furukawa	RCNP
W.H. Guo	RCNP-Toyonaka
A. Inoue	RCNP
R. Iwasaki	RCNP-Toyonaka
N. Kobayashi	RCNP
M. Murata	RCNP
S. Ota	RCNP
Y. Sasagawa	RCNP-Toyonaka
H. Shibakita	RCNP-Toyonaka
J. Tanaka	RCNP
T. Furuno	Dep. Phys., Osaka Univ.
Y. Honda	Dep. Phys., Osaka Univ.
T. Kawabata	Dep. Phys., Osaka Univ.
T. Okamura	Dep. Phys., Osaka Univ.
K. Sakanashi	Dep. Phys., Osaka Univ.
H. Shimojo	Dep. Phys., Osaka Univ.
Y. Fujikawa	Kyoto Univ.
S. Okamoto	Kyoto Univ.
A. Adachi	CYRIC, Tohoku Univ.
J.A.C. Bekker	Wits and iThemba LABS
S.D. Binda	Wits and iThemba LABS
J.W. Brummer	iThemba LABS
L.M. Donaldson	iThemba LABS
L. Jafta	iThemba LABS and Univ. Western Cape
P.M. Jones	iThemba LABS
S. Jongile	iThemba LABS and Stellenbosch Univ.
T. Khumalo	Wits and iThemba LABS
S. Magagula	Wits and iThemba LABS
K.L. Malatji	iThemba LABS
R. Molaeng	Wits and iThemba LABS
R. Neveling	iThemba LABS
A. Netshiya	Wits and iThemba LABS
E. Sideras-Haddad	Univ. Witwatersrand
S. Triambak	Univ. Western Cape
M. Wiedeking	Berkeley National Laboratory and Wits
D. Balabanski	ELI-NP
E. Boicu	ELI-NP
M. Brezeanu	ELI-NP
A. Gavrilescu	ELI-NP
A. Kuşoğlu	ELI-NP
T. Petruse	ELI-NP
I. Brandherm	IKP, Tech. Univ. Darmstadt
J. Isaak	IKP, Tech. Univ. Darmstadt
I. Jurosevic	IKP, Tech. Univ. Darmstadt
J. Kleemann	IKP, Tech. Univ. Darmstadt
P. von Neumann-Cosel	IKP, Tech. Univ. Darmstadt
N. Pietralla	IKP, Tech. Univ. Darmstadt
O. Papst	IKP, Tech. Univ. Darmstadt
M. Spall	IKP, Tech. Univ. Darmstadt
V. Werner	IKP, Tech. Univ. Darmstadt
A. Bracco	Univ. Milano/INFN
F. Camera	Univ. Milano/INFN
F. Crespi	Univ. Milano/INFN
A. Giaz	INFN-Milano/Univ. Milano
O. Wieland	INFN-Milano
J.K. Dahl	Univ. Oslo
J.M.W. Finsrud	Univ. Oslo
A. Görgen	Univ. Oslo
V.W. Ingeberg	Univ. Oslo
K.C.W. Li	Univ. Oslo
E.M. Martinsen	Univ. Oslo
W. Paulsen	Univ. Oslo
S. Siem	Univ. Oslo
Cheng Wang	Peking Univ.
Zaihong Yang	Peking Univ.
Kaijie Zhou	Peking Univ.
P. Adsley	Texas A&M Univ.
M.S. Reen	Akal Univ.
Y. Koshio	Okayama Univ.
T. Suda	ELPH, Tohoku Univ..
H. Utsunomiya	Shanghai Adv. Res. Inst.
H. Wang	Shanghai Adv. Res. Inst.
F.Y.A. Limonge	Univ. de Santiago de Compostela

Nuclear Theory:

R. Dalal	Guru Jambheshwar Univ.
S. Goriely	Univ. Bruxelles
T. Inakura	Tokyo Institute of Technology
E. Khan	IJCLab, Orsay
M. Kimura	RIKEN & Hokkaido Univ.
E. Litvinova	West Michigan Univ.
H. Motoki	Hokkaido Univ.
P. Ring	TU-Munich
N. Shimizu	Tsukuba Univ.
Y. Taniguchi	Kagawa College
N. Tsoneva	ELI-NP
Y. Utsuno	Japan Atomic Energy Agency
H. Wibowo	Univ. York
Y. Xu	ELI-NP

UHECR:

D. Allard	CNRS, Univ. Paris
B. Baret	CNRS, Univ. Paris
I. Deloncle	IJCLab, Orsay
H. Haoning	RIKEN
R. Higuchi	RIKEN
O. Just	RIKEN
E. Kido	RIKEN
J. Kiener	IJCLab, Orsay
S. Nagataki	RIKEN
J. Oliver	RIKEN
E. Parizot	IJCLab, Orsay
V. Tatischeff	IJCLab, Orsay

PANDORA project: experimental facilities

Photo-**A**bsorption of **N**uclei and **D**ecay **O**bservation for **R**eactions in **A**strophysics

White paper: AT et al.,. Euro. Phys. J. A **59**, 208 (2023)

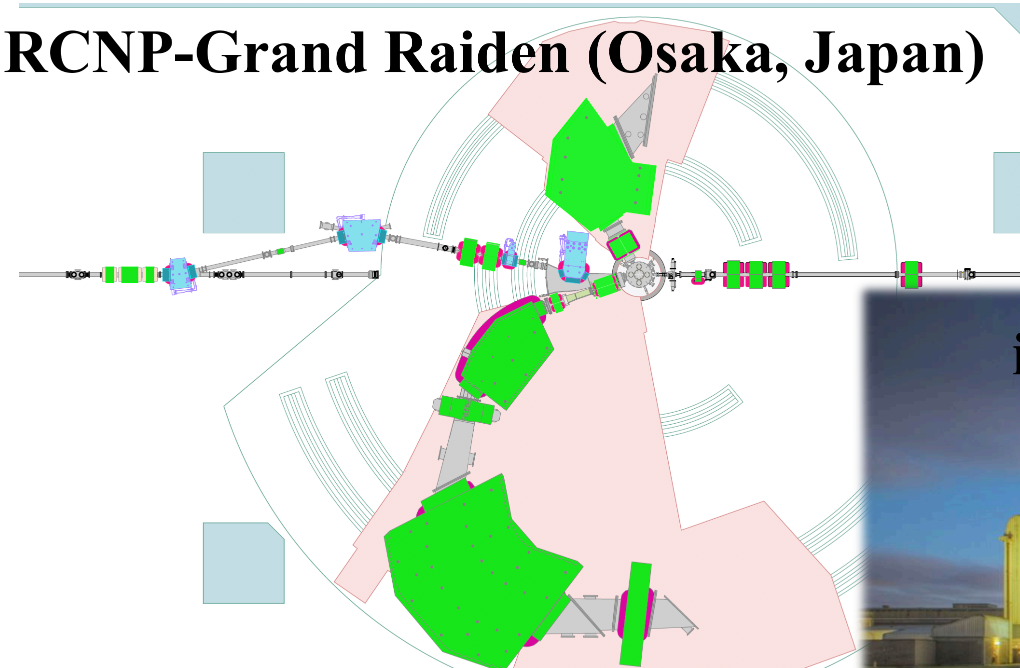

Experiments at three facilities with complementary techniques

Joint project of experimental nuclear physics, theoretical nuclear physics and particle astrophysics

Experiment combining three complementary facilities

Virtual Photon Exp.

iThemba LABS **2024-** ^{12}C and ^{27}Al

Total strength distribution up 24 MeV

p,α,γ-decays

multipole decomp. analysis

iThemba LABS, Univ. Witwatersland, Stellenbosh Univ.

L. Pellegri, R. γ, F.D. Smit, J.A.C. Bekker, S. Binda, H, Jivan, T. Khumal, M. Wiedeking, K.C.W. Li, P. Adsley, L.M. Donaldson, E. Sideras-Haddado, K.L. Malatji, S. Jongile, A. Netshiya

RCNP **2023-** (^{10,11}B), ^{12,13}C, ^{24,26}Mg, ^{27}Al

Total strength distribution up 32 MeV

p,α,γ-decays

multipole decomp. analysis

Osaka Univ.

A. Tamii, N. Kobayashi, T. Sudo, M. Murata, A. Inoue, **R. Niina**, T. Kawabata, T. Furuno, S. Adachi, K. Sakanashi, K. Inaba, Y. Fujikawa, S. Okamoto, Y. Fujita, H. Fujita

Real Photon Exp.

ELI-NP 2025-

absolute c.s.

model independent separation of E1 and M1

n,p,α,γ-decays up to 20 MeV

ELI-NP

P.-A. Söderström, D. Balabanski, L. Capponi, A. Dhal, T. Petruse, D. Nichita, Y. Xu

Probes for the Electric Dipole Response of Nuclei

1. Virtual photon excitation
   (Coulomb excitation)
   - proton inelastic scattering at 0 deg.

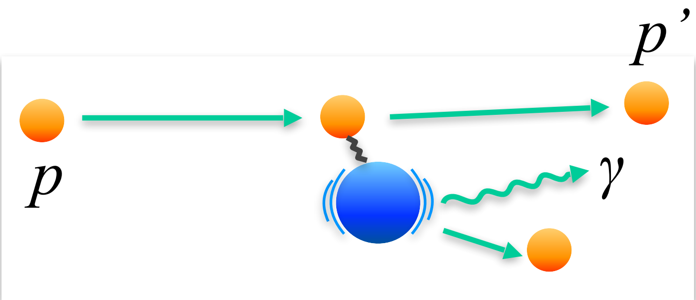

Proton beams at RCNP and iThemba LABS

E_x distribution in one shot measurement
total photo-absorption c.s.
up to 32 (24) MeV at RCNP (iThemba)

2. Real photon absorption
   - (γ,γ') Nuclear Resonance Fluorescence
   - (γ,n), (γ,2n), (γ,p), … photodisintegrations

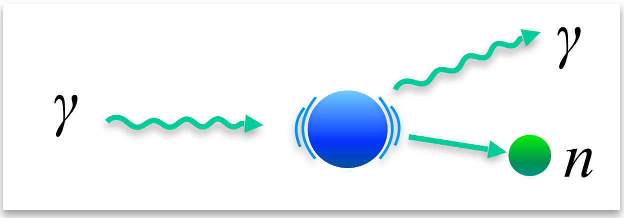

Real γ-beam at ELI-NP

pure EM probe
precise absolute c.s.
partial strength including *n*
up to 20 MeV at ELI-NP

Experimental Setup (established in E563)

Measurement at **0 deg.**

0-deg transmission mode

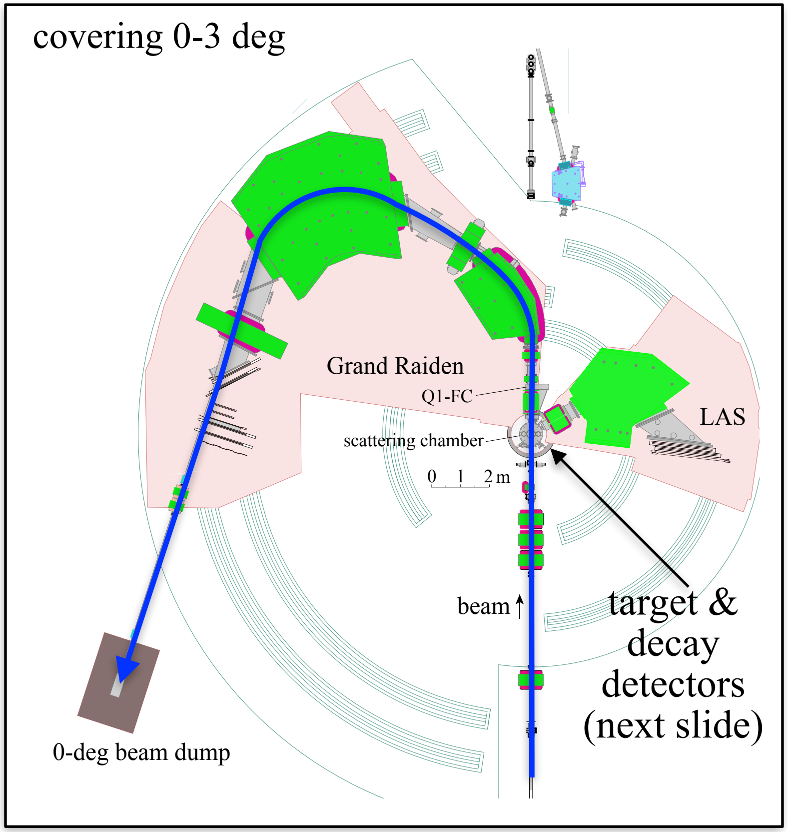

Measurement at **4.5** and **6.6 deg.**

GRAF mode

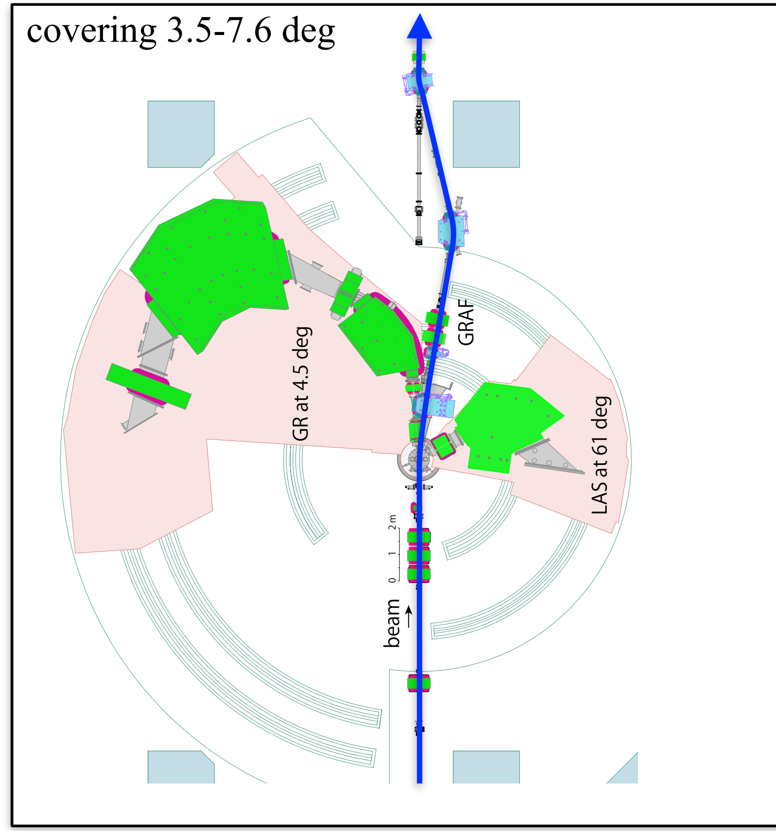

proton beam at 392 MeV

30 mg/cm² targets for inclusive cross sections (σ_{abs})

1 mg/cm² targets for charged particle decay coincidence

Decay Particle Detectors

SAKRA in PANDORA Scat. Chamber

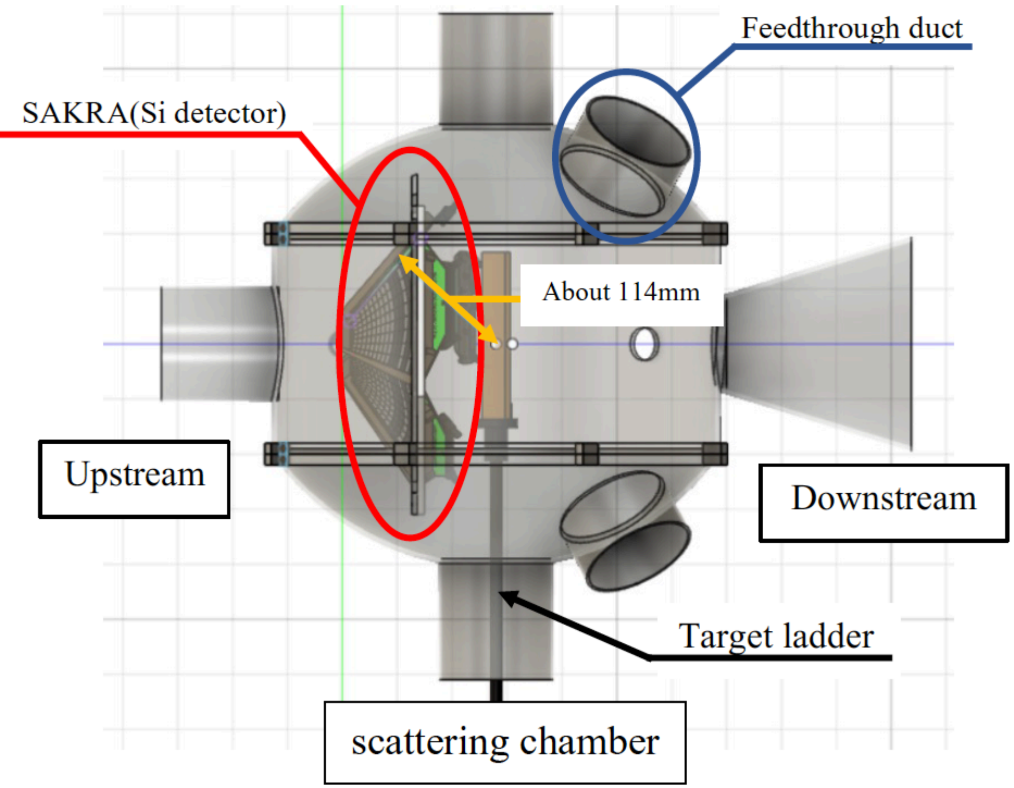

Scγlla setup

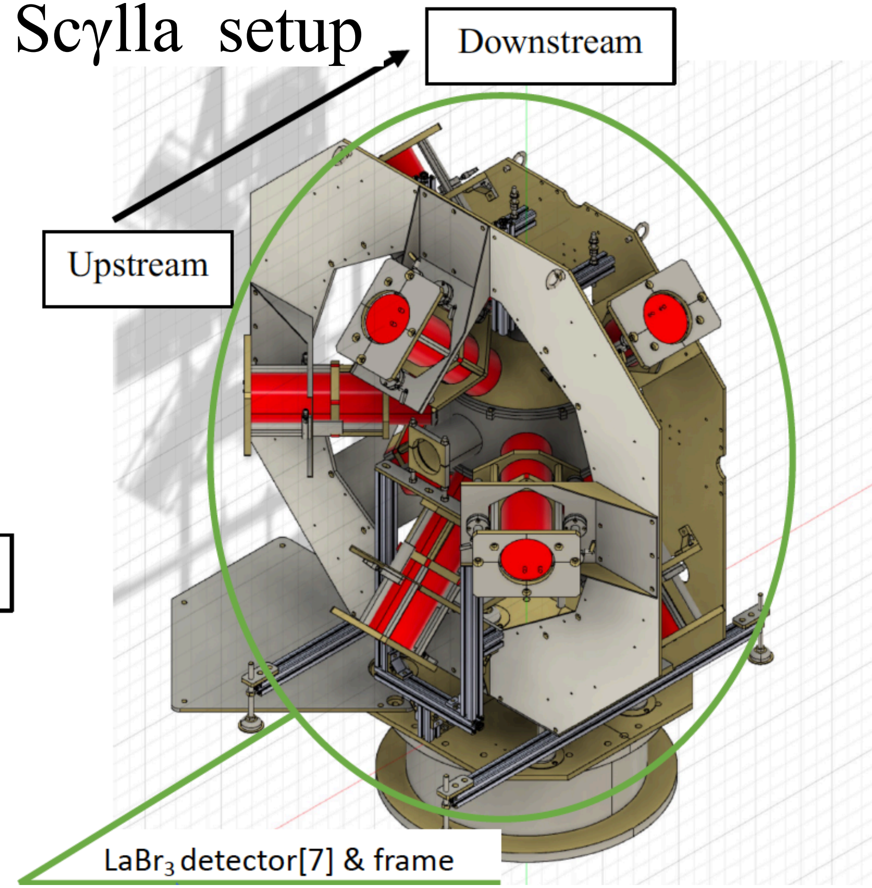

5 pairs of DSSSD detectors (SAKRA) for decay charged particles

8 large volume LaBr3 detectors from Milano for decay gamma-rays

Experimental setup, E563, September-October, 2023

SCγLLA

Milano-LaBr3

SAKRA DSSSDs

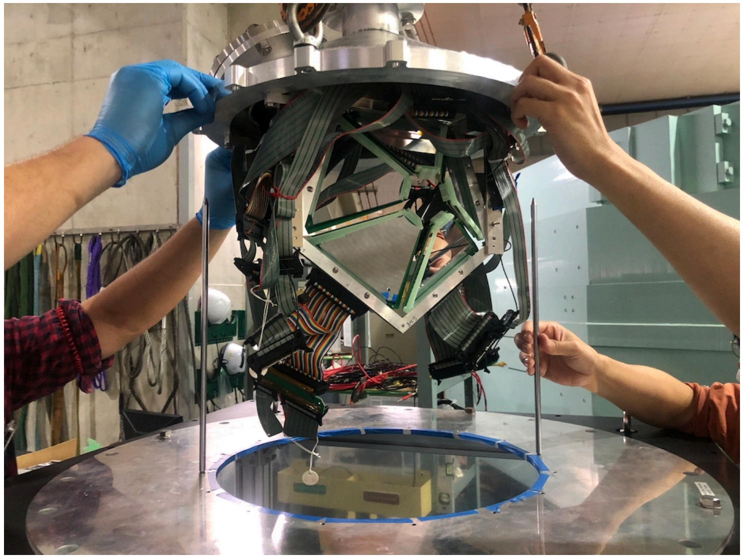

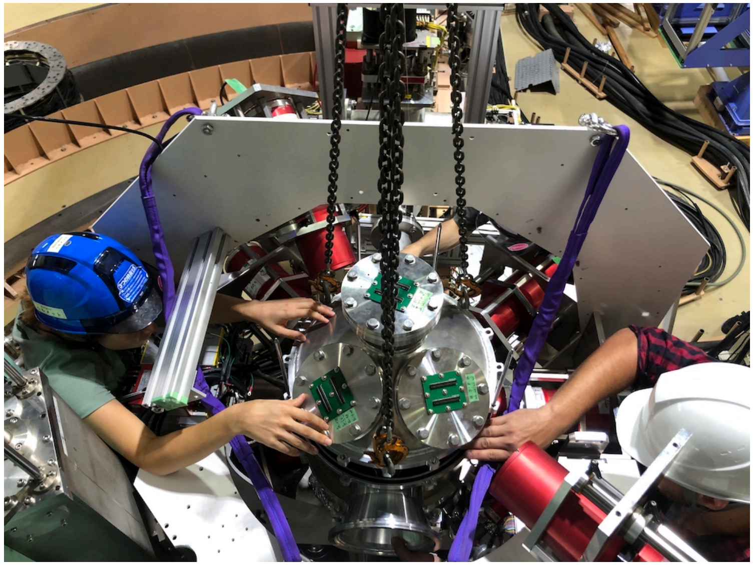

51 visiting collaborators: 36 (abroad) + 15 (Japan)

Preliminary data from E563

Data analysis by J.A.C. Bakker and Y. Sasagawa

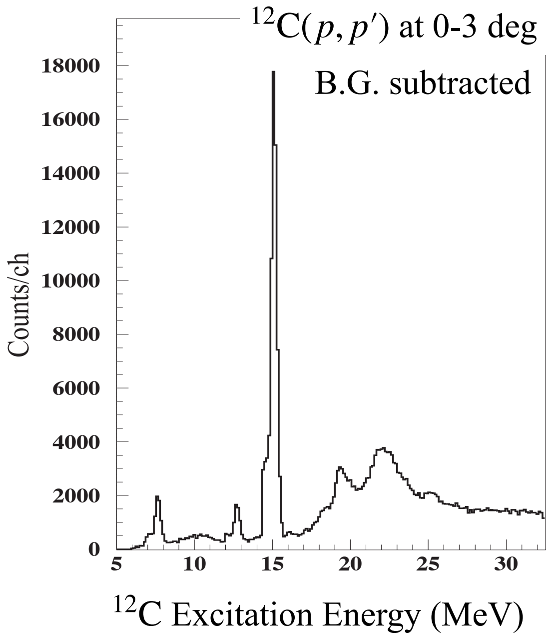

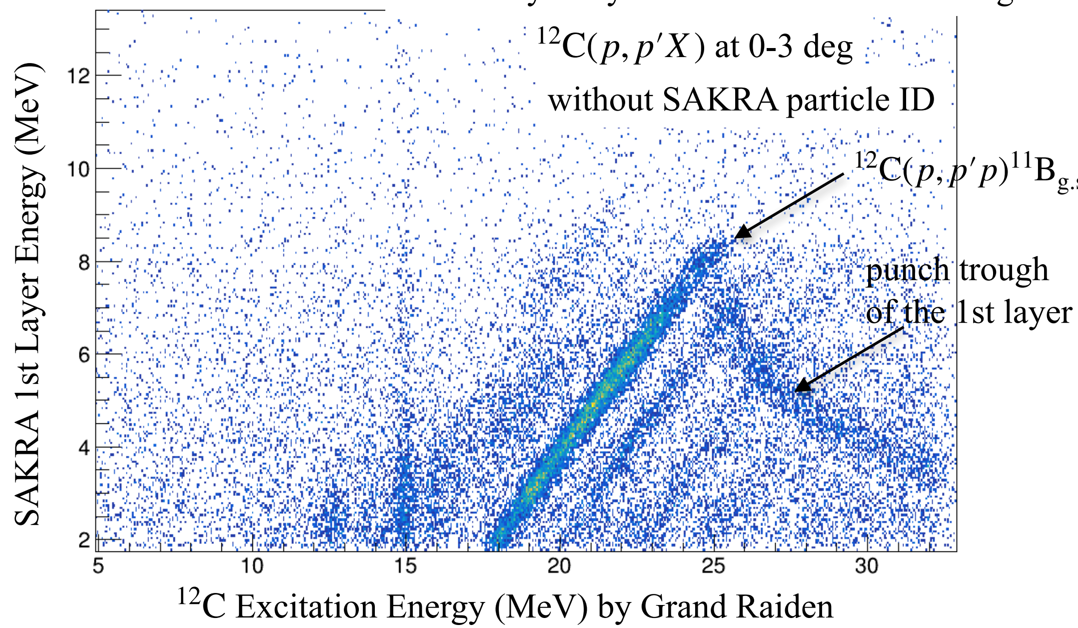

SAKRA particle ID (calibration in progress)

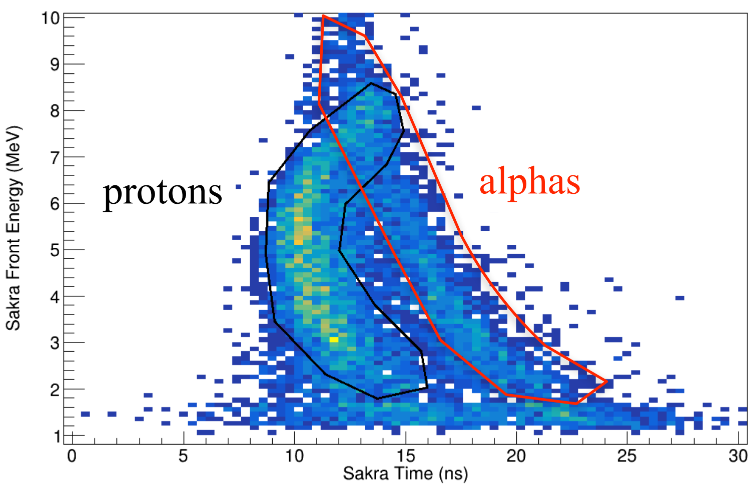

Better separation of p and α is anticipated after calibration of the flight length

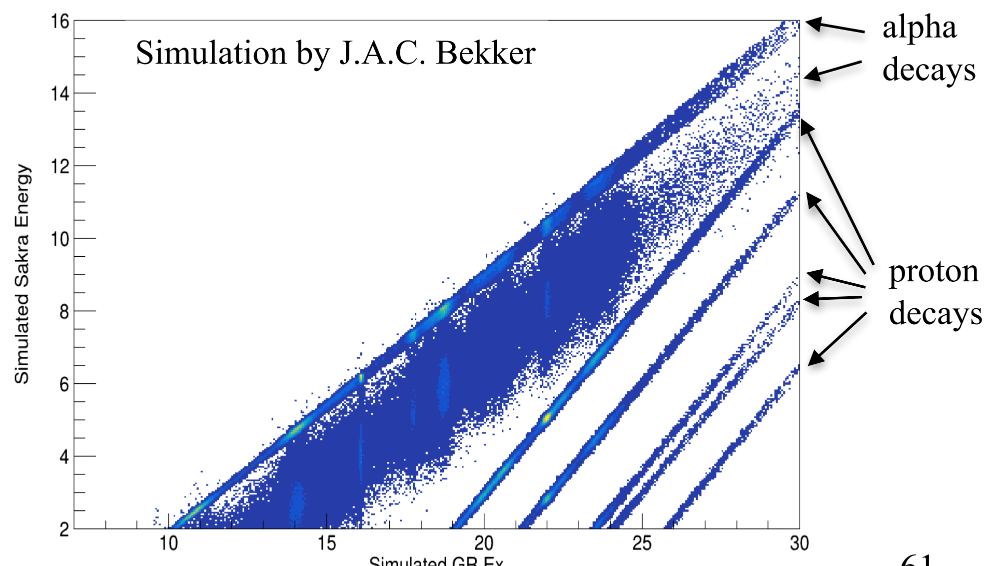

Predictions

AMD + Laplace Expansion (M. Kimura et al.,)

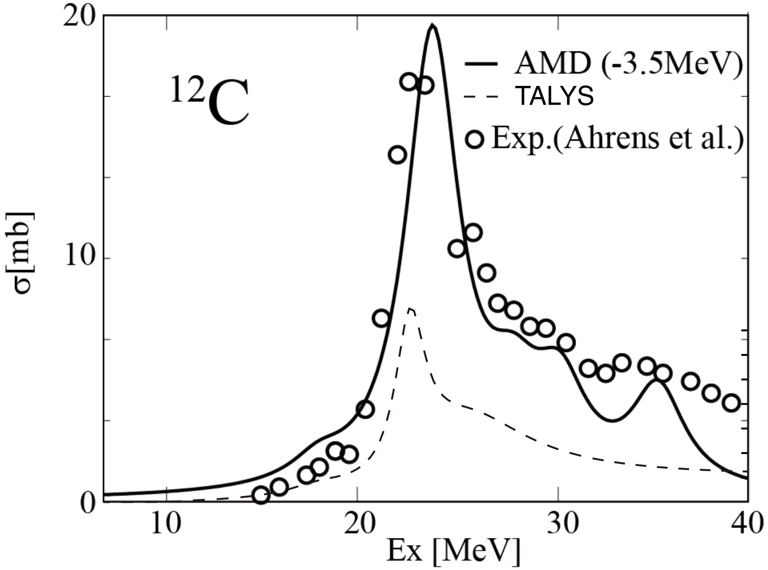

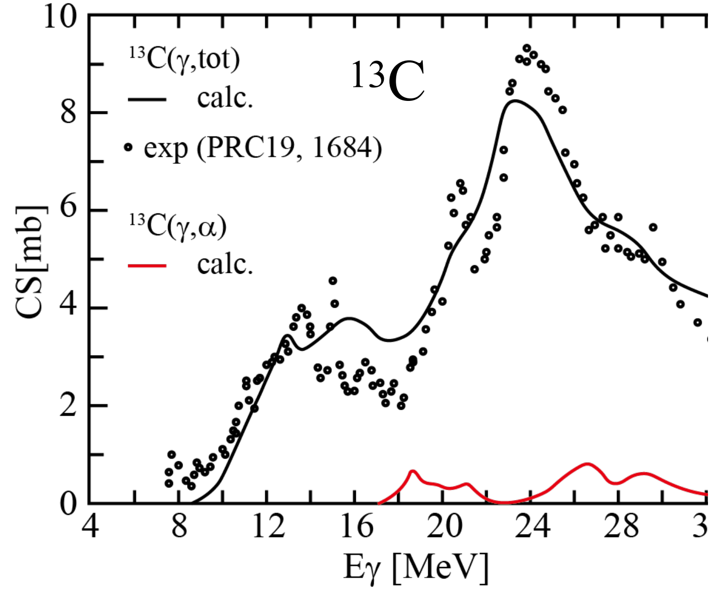

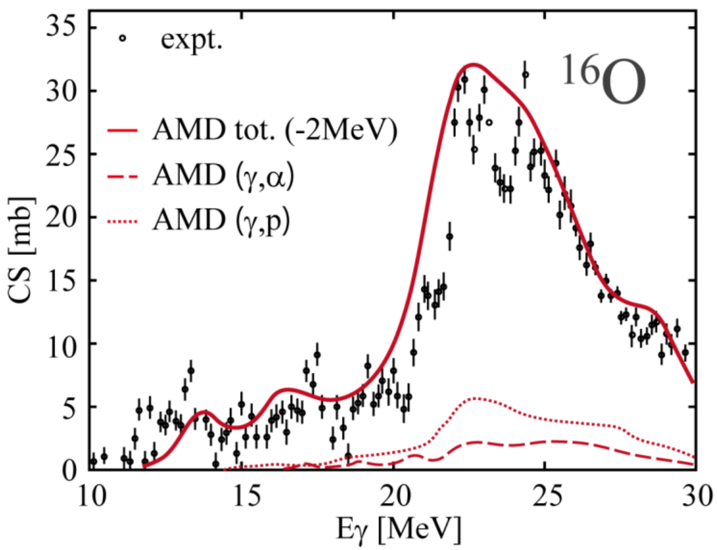

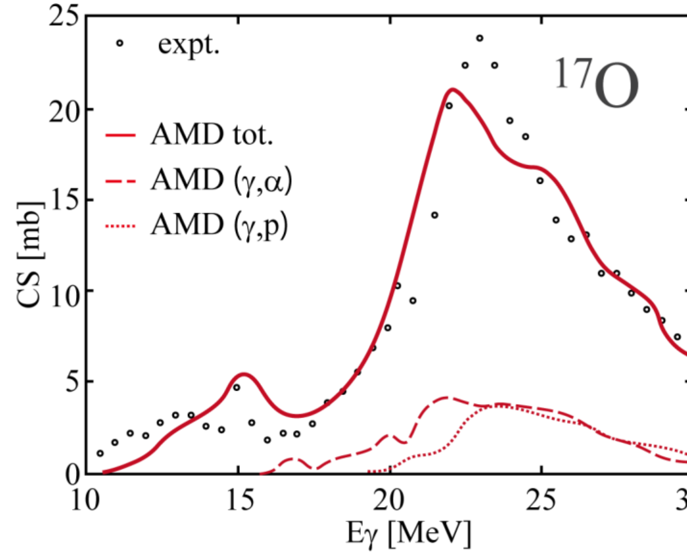

Theoretical Model Developments

AMD + Laplace Expansion (M. Kimura et al.,)

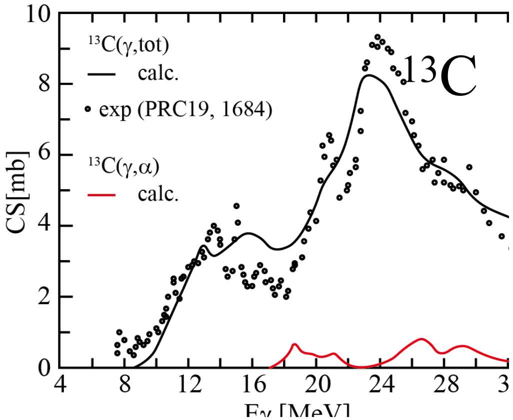

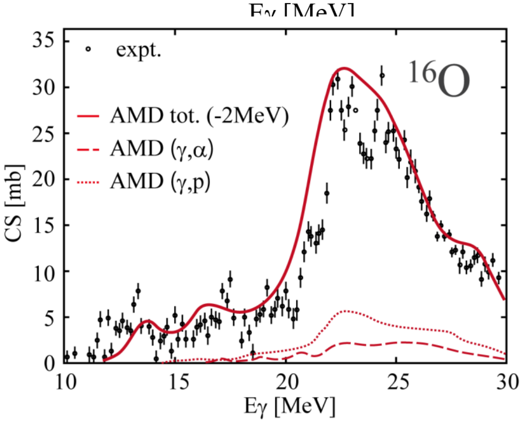

Isospin mixing and selection rule

M. Kimura et al., arXiv:2108.07592 (2021)

RPA by T. Inakura

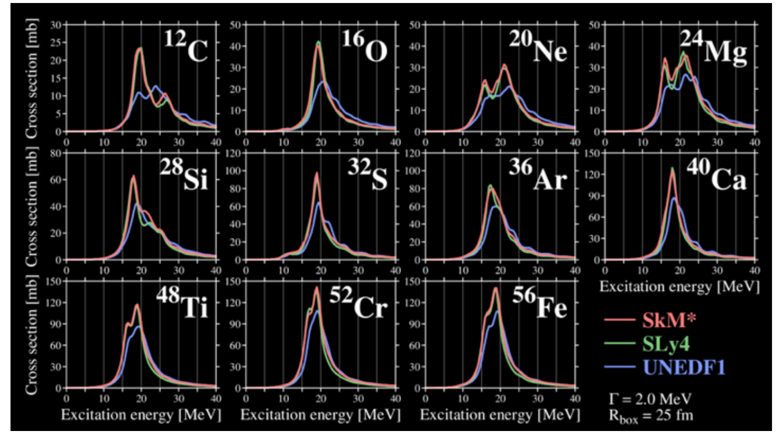

N. Shimizu, Y. Utsuno, et al.,

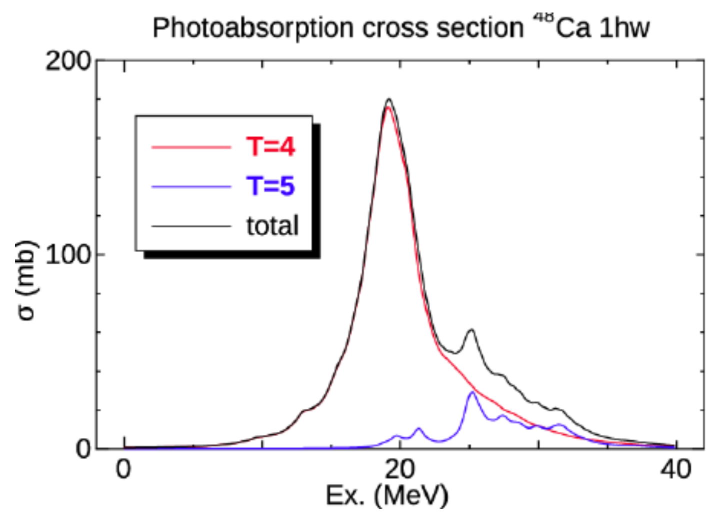

Development of theoretical models is inevitable to make predictions for all the relevant nuclei.

It is important to evaluate the uncertainty of the model predictions.